CAPITAL UNIVERSITY OF SCIENCE AND TECHNOLOGY, ISLAMABAD

Determination of *Aloe barbadensis Miller* Active Constituents against Cathelicidin *LL-37* to Cure Rosacea an *Insilico* Study

by

Ayesha Bukhari

A thesis submitted in partial fulfillment for the degree of Master of Science

in the

Faculty of Health and Life Sciences
Department of Bioinformatics and Biosciences

2025

I dedicate this thesis to my loving and supportive family who have fully helped me in achieving my life goals.

CERTIFICATE OF APPROVAL

Determination of *Aloe barbadensis Miller* Active Constituents against Cathelicidin *LL-37* to Cure Rosacea an *Insilico* Study

by

Ayesha Bukhari

(MBS241014)

THESIS EXAMINING COMMITTEE

S. No.	Examiner	Name	Organization
(a)	External Examiner	Dr. Rehana Rani	NUST, Islamabad
(b)	Internal Examiner	Dr. Sohail Ahmad Jan	CUST, Islamabad
(c)	Supervisor	Dr. Erum Dilshad	CUST, Islamabad

Dr. Erum Dilshad
Thesis Supervisor
September, 2025

Dr. Syeda Marriam Bakhtiar
Head
Dept. of Bioinfo. & Biosciences
September, 2025

Dr. Sahar Fazal
Dean
Faculty of Health & Life Sciences
September, 2025

Author's Declaration

I, **Ayesha Bukhari** hereby state that my MS thesis titled "**Determination of *Aloe barbadensis Miller* Active Constituents against Cathelicidin *LL-37* to Cure Rosacea an *Insilico* Study**" is my own work and has not been submitted previously by me for taking any degree from Capital University of Science and Technology, Islamabad or anywhere else in the country/abroad.

At any time if my statement is found to be incorrect even after my graduation, the University has the right to withdraw my MS Degree.

(Ayesha Bukhari)

Registration No: MBS241014

Plagiarism Undertaking

I solemnly declare that research work presented in this thesis titled "**Determination of *Aloe barbadensis Miller* Active Constituents against Cathelicidin *LL-37* to Cure Rosacea an *Insilico* Study**" is solely my research work with no significant contribution from any other person. Small contribution/help wherever taken has been duly acknowledged and that complete thesis has been written by me.

I understand the zero tolerance policy of the HEC and Capital University of Science and Technology towards plagiarism. Therefore, I as an author of the above titled thesis declare that no portion of my thesis has been plagiarized and any material used as reference is properly referred/cited.

I undertake that if I am found guilty of any formal plagiarism in the above titled thesis even after award of MS Degree, the University reserves the right to withdraw/revoke my MS degree and that HEC and the University have the right to publish my name on the HEC/University website on which names of students are placed who submitted plagiarized work.

(Ayesha Bukhari)
Registration No: MBS241014

Acknowledgement

All praise and thanks to the Supreme God to whom we only bow down. I would also like to express my gratitude to my family and friends for their continuous mental and physical support and prayers. I would also wholeheartedly say a big thank you to my supervisor Dr. Erum Dilshad (Associate Professor, Department of Bioinformatics and Biosciences, CUST) for her support and for giving his precious time to assist with computational approaches.

(Ayesha Bukhari)

Abstract

Rosacea is a chronic inflammatory dermatosis characterized by facial redness, papules, pustules, and vascular dysregulation. One of the central factors in its pathogenesis is the overexpression of the antimicrobial peptide cathelicidin (LL-37), which activates inflammatory pathways via the NLRP3 inflammasome. This study aimed to identify potential plant-derived inhibitors of LL-37 using compounds isolated from *Aloe barbadensis Miller* (*Aloe Vera*). The 3D structure of LL-37 (PDB ID: 2K6O) was retrieved and refined using PyMOL, and its physicochemical properties and functional domains were characterized using ProtParam and InterPro, respectively. Twenty-five phytochemicals including flavonoids (Apigenin, Quercetin, Kaempferol), anthraquinones (Aloe emodin, Chrysophanic acid), polysaccharides (Glucomannan), phenolic acids, steroids, terpenes, and vitamins were sourced from PubChem, energy minimized with Chem3D, and subjected to molecular docking against LL-37 using CB-Dock (AutoDock Vina). The resulting docking scores and cavity sizes were analyzed, and ligand–protein interactions were visualized via PyMOL and LigPlot. Drug-likeness was assessed using Lipinski's Rule of Five, followed by pkCSM-based ADMET (Absorption, Distribution, Metabolism, Excretion, and Toxicity) profiling.

Among the 25 compounds, the strongest docking scores were exhibited by Isoaloeresin D (-6.6 kcal/mol), Folic Acid (-6.3 kcal/mol), Vitamin E acetate (-6.2 kcal/mol), and Lupeol and Campesterol (-5.9 kcal/mol). However, several of these top-scoring candidates were disqualified due to violations of Lipinski's rule or unfavorable ADMET profiles, including poor water solubility, high molecular weight, hERG II inhibition, low intestinal absorption, or excessive lipophilicity (LogP ¿ 7). In contrast, Apigenin emerged as the most promising lead compound, showing a good docking score (-5.1 kcal/mol), full compliance with Lipinski's Rule, and excellent ADMET characteristics including high human intestinal absorption (93.25%), no predicted hepatotoxicity, non-mutagenicity, absence of P-glycoprotein interaction, and moderate clearance (0.566 mL/min/kg). Kaempferol and Quercetin also demonstrated favorable docking affinities (-5.1 kcal/mol) and safety profiles,

though with slightly less optimal pharmacokinetic parameters compared to Apigenin.

When compared to the reference drug Doxycycline, which had a slightly better docking score (-5.8 kcal/mol), Apigenin showed superior drug-likeness and ADMET characteristics. Doxycycline had lower intestinal absorption (44.5%) and was flagged as a P-glycoprotein substrate, indicating potential drug-efflux and lower bioavailability. Additionally, Doxycycline presented a more complex hydrogen bonding profile, potentially limiting its membrane permeability. Overall, Apigenin was identified as the most viable candidate due to its balanced efficacy, safety, and pharmacokinetic advantages. Kaempferol and Quercetin remain strong secondary candidates. This study highlights the therapeutic potential of natural anti-inflammatory compounds from *Aloe vera* in targeting LL-37 for rosacea treatment and supports further *in vitro* and *in vivo* investigations to validate Apigenin as a clinical lead.

Keywords: Rosacea, Cathelicidin (LL-37), Inflammation, *Aloe vera*, Molecular docking, Antimicrobial peptides, *In silico* analysis, Skin disease, Bioactive compounds

Contents

List of Figures

List of Tables

Chapter 1

Introduction

Rosacea is a chronic inflammatory skin disorder that mainly affects the central areas of the face, such as the nose, cheeks, chin, and forehead. It is marked by repeated episodes of facial flushing, persistent redness (erythema), visible blood vessels (telangiectasia), and the appearance of papules and pustules [1].

It primarily affects adults aged 30 to 60 and is more commonly seen in individuals with fair skin. Historically, rosacea was often misdiagnosed as acne due to similar presentations. Over time, it has been recognized as a distinct dermatological condition, leading to more targeted research and treatment approaches.

The exact etiology of rosacea remains unclear, several factors have been implicated [2]. Genetics Predisposition that is defined as A higher incidence in individuals with a family history suggests a genetic component [3]. Immune System Deregulation that is defined as Abnormal immune responses may contribute to inflammation. Neurovascular Deregulation that is defined as Recent studies highlight the role of neurovascular components in rosacea's pathogenesis, leading to symptoms like intense redness [2].

There are many therapies such as Topical Therapies that is a type of Metronidazole and azelaic acid remain standard treatments. Recent advancements include the exploration of natural compounds like artemisinin, derived from Artemisia annua, which has demonstrated anti-inflammatory and anti-angiogenic properties

beneficial for rosacea management [4]. and oral antibodies Low-dose doxycycline is commonly prescribed for its anti-inflammatory effects. The FDA recently approved Emrosi (DFD-29), a low-dose minocycline, showing significant efficacy in reducing inflammatory lesions and facial redness.

Cathelicidins, particularly the antimicrobial peptide LL-37, are integral to the skin's innate immune defense. In rosacea patients, elevated levels of cathelicidin and increased activity of serine proteases, such as stratum corneum tryptic enzyme (SCTE), have been observed. These enzymes abnormally process cathelicidin into pro-inflammatory peptides, leading to the characteristic inflammation, erythema in rosacea [5]. Mast cells have been identified as key mediators in this inflammatory cascade. They release proteases that not only recruit other immune cells but also contribute to vasodilation and angiogenesis, exacerbating symptoms [6].

Additionally, a positive feedback loop between the mechanistic target of rapamycin complex 1 (mTORC1) and cathelicidin has been implicated in promoting skin inflammation in rosacea. This loop suggests that mTORC1 activation enhances cathelicidin expression, which in turn sustains mTORC1 activity [7].

Elevated levels of LL-37 in rosacea patients have been linked to increased inflammation and vascular changes. This peptide enhances photosensitivity, augmenting the pro-inflammatory and pro-angiogenic effects of ultraviolet (UV) radiation, leading to the release of interleukin-1β (IL-1β) [8].

Aloe vera (*Aloe barbadensis miller*) is known for its anti-inflammatory, antimicrobial, and skin-soothing properties. Its active compounds, such as aloesin and acemannan, have demonstrated potential in modulating inflammatory pathways. Specifically, *Aloe vera* inhibits cyclooxygenase activity.

Recent studies have highlighted role of cathelicidin (LL-37) in pathogenesis of rosacea, particularly its ability to activate the NLRP3 inflammasome, leading to increased inflammation [9].

In silico investigations have been employed to identify potential inhibitors targeting LL-37 and interleukin-8 (IL-8), both of which are implicated in rosacea's inflammatory processes. These computational studies utilize molecular docking

and dynamics simulations to predict how small molecules might interact with these targets, offering a cost-effective approach to drug discovery [10].

Additionally, botulinum toxin (BoNT) has been explored as a treatment option for rosacea. BoNT appears to reduce LL-37-induced erythema by inhibiting mast cell degranulation, thereby decreasing inflammation associated with rosacea [11].

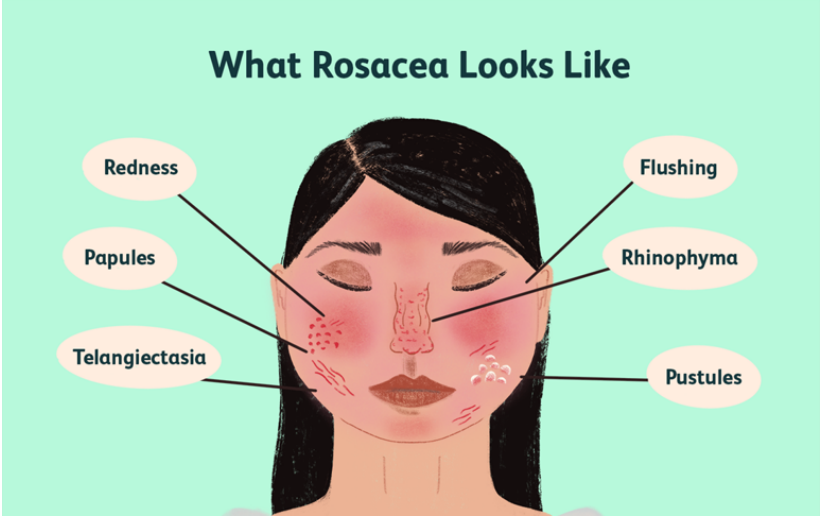

FIGURE 1.1: Roseasea [1]

1.1 Problem Statement

Rosacea is a chronic inflammatory skin disorder with limited targeted therapies. Cathelicidin (LL-37) drives its pathogenesis by inducing inflammation and immune responses, while conventional treatments show limited efficacy and side effects. Hence, novel natural compounds are needed. Aloe vera, rich in anti-inflammatory and skin-healing constituents, is a promising candidate. This study employs in silico approaches to explore Aloe vera's active compounds against LL-37, aiming for an effective and safer therapeutic strategy for rosacea.

1.2 Aim and Objectives

- The main aim of this study is to predict potential inhibitors against roseasea by the use of molecular docking of active compounds of alovera showing

antinflamatory properties with cathelicidin (LL-37) to treat rosacea.

The objectives of the study include:

- To identify probable inhibitory compounds with anti-inflamatoy properties present in alovera against cathelicidin (LL-37) of rosacea.
- To analyze the interaction between ligand and protein complex by performing molecular docking.
- To find the best of the interacting molecules that shows inhibitory effects against the roseasea.

1.3 Scope

In silico molecular docking presents a valuable approach for identifying inhibitory compounds targeting cathelicidin (LL-37) is a key antimicrobial peptide implicated in pathogenesis of rosacea disease. Dysregulated expression and processing of LL-37 contribute to inflammation, erythema, and vascular abnormalities characteristic of the disease. By screening potential inhibitors, molecular docking can aid in the discovery of novel therapeutic compounds capable of modulating LL-37 activity, thereby mitigating inflammatory responses. This computational strategy could accelerate drug development efforts, offering targeted interventions to combat rosacea more effectively.

Chapter 2

Literature Review

2.1 Rosacea Skin Disease

Over the last 15 years, a wide range of clinical, epidemiological, and pathophysiological studies have been conducted on rosacea. This chronic inflammatory skin disease mainly affects the central facial area and is marked by persistent redness, papules, pustules, and visible blood vessels (telangiectasia). Its development is linked to a combination of genetic predisposition, immune system abnormalities, and various environmental triggers. Recent research emphasizes the involvement of a dysregulated innate immune response, significant vascular alterations, and increased colonization by Demodex mites. Common aggravating factors include exposure to ultraviolet (UV) radiation, extreme temperatures, certain foods, and specific medications [12].

Causes Genetic predisposition plays a significant role, as evidenced by higher concordance rates in twins and familial aggregation of the condition. Environmental factors, such as ultraviolet radiation, extreme temperatures, and certain dietary components, can exacerbate rosacea symptoms by inducing vasodilation and inflammatory responses. Microbial involvement, particularly the proliferation of *Demodex folliculorum* mites and the presence of Helicobacter pylori infection, has been implicated in the pathogenesis of rosacea. These microorganisms may trigger immune responses leading to inflammation and vascular changes characteristic of

the disease. Additionally, dysregulation of the innate immune system, including overexpression of cathelicidins and matrix metalloproteinases, contributes to the inflammatory milieu observed in rosacea patients. Neurovascular dysregulation, resulting in increased blood flow and vessel permeability, further exacerbates the condition [16].

Epidemiological data show that rosacea affects approximately 5.46% of the global adult population, with its prevalence increasing notably with age [13]. A population-based study of 161,269 individuals found a prevalence of 0.3% among those aged 16–29 years, which rose to 5.7% in people aged 60–70 years. Rosacea is also more common in individuals with fair skin, particularly those of Northern European ancestry [14]. Clinically, rosacea is characterized by facial redness, visible blood vessels, and inflammatory lesions, all of which can significantly affect a patient's quality of life. Ocular rosacea, which involves eye irritation, is frequently underdiagnosed due to its nonspecific symptoms [15].

Diagnosis is primarily clinical, based on typical skin findings and patient history, as there are no specific laboratory tests for rosacea. Management includes both pharmacologic and non-pharmacologic approaches, tailored according to disease severity and subtype. Common treatments include topical agents like metronidazole and azelaic acid, and oral antibiotics such as doxycycline for their anti-inflammatory effects. Laser and light-based therapies have also proven effective in reducing redness and telangiectasia [12].

Avoiding personal triggers and maintaining an appropriate skincare routine are crucial for effective management. Moreover, recent studies suggest possible links between rosacea and systemic conditions, including autoimmune diseases, highlighting the need for a comprehensive, patient-centered treatment approach.

2.2 Causes

Genetic predisposition plays a significant role, as evidenced by higher concordance rates in twins and familial aggregation of the condition. Environmental

factors, such as ultraviolet radiation, extreme temperatures, and certain dietary components, can exacerbate rosacea symptoms by inducing vasodilation and inflammatory responses. Microbial involvement, particularly the proliferation of *Demodex folliculorum* mites and the presence of Helicobacter pylori infection, has been implicated in the pathogenesis of rosacea. These microorganisms may trigger immune responses leading to inflammation and vascular changes characteristic of the disease. Additionally, dysregulation of the innate immune system, including overexpression of cathelicidins and matrix metalloproteinases, contributes to the inflammatory milieu observed in rosacea patients. Neurovascular dysregulation, resulting in increased blood flow and vessel permeability, further exacerbates the condition [16].

2.3 Life Cycle

It starts with Initiation Phase in which the development of rosacea is often triggered by various environmental and endogenous factors, including ultraviolet (UV) radiation, heat, emotional stress, and certain microorganisms. These stimuli can activate the innate immune system, particularly through toll-like receptor 2 (TLR2), leading to an exaggerated inflammatory response [17]. Then Microbial Factors in which an increased density of *Demodex folliculorum* mites has been observed in individuals with rosacea. These mites may harbor Bacillus oleronius, a bacterium that can stimulate TLR2, further amplifying the inflammatory response [18]. The Activation of TLR2 leads to the upregulation of kallikrein 5 (KLK5), a serine protease that processes cathelicidin (LL-37), an antimicrobial peptide. In rosacea patients, this pathway is dysregulated, resulting in the production of pro-inflammatory LL-37 fragments. These fragments induce vasodilation, inflammation, and matrix degradation, contributing to the clinical manifestations of rosacea [19]. Persistent inflammation can result in tissue remodeling, leading to phymatous changes and fibrosis observed in advanced stages of rosacea. The interplay between immune responses, microbial factors, and neurovascular dysregulation contributes to the chronicity and progression of the disease [20].

2.4 Prevalence

Its prevalence varies globally, influenced by different factors such as geographic location, diagnostic criteria, and study methodologies. A systematic review as well as meta-analysis estimated that approximately 5.46% of the global adult population is affected by rosacea [13]. In Germany, a study reported a prevalence of 12.3%, while in Russia, it was 5.0% [21]. Data from the United Kingdom indicate an incidence rate 1.65 per 1,000 person-years, with diagnoses predominantly occurring after the age of 30 [22]. Notably, rosacea prevalence increases with age, rising from 0.3% in individuals aged 16-29 to 5.7% in those aged 60-70 [14].

2.5 Symptoms

Rosacea is a long-standing inflammatory skin disorder that primarily affects the central areas of the face, such as the forehead, nose, cheeks, and chin Clinical presentations of rosacea vary and are classified into specific subtypes based on dominant features. The erythematotelangiectatic subtype is characterized by persistent facial redness and visibly dilated blood vessels (telangiectasia). The papulopustular subtype presents with temporary or continuous redness along with inflammatory papules and pustules. Phymatous rosacea is marked by skin thickening and an uneven, nodular surface, most commonly affecting the nose and resulting in rhinophyma. Ocular rosacea manifests as ocular discomfort, including dryness, irritation, and eyelid inflammation. Common symptoms across these subtypes include facial flushing, burning or stinging sensations, and increased skin sensitivity. These symptoms can significantly impact patients' quality of life, leading to emotional distress and social avoidance [23].

2.6 Diagnosis

The diagnosis of skin disease (roseasea) is primarily clinical, relying on the identification of these characteristic features during a thorough patient history and

physical examination. According to updated guidelines, a diagnosis can be established. The diagnosis is supported by the presence of either phymatous changes or persistent Centro facial erythema. If these primary features are absent, the presence of at least two secondary features such as flushing, papules and pustules, telangiectasia, or ocular involvementcan also confirm the diagnosis [24]. Recent advancements emphasize a phenotype-based approach to diagnosis, focusing on the identification of individual clinical features rather than traditional subtyping. This approach facilitates personalized treatment strategies and acknowledges the heterogeneous nature of rosacea presentations [25].

2.7 Treatment

Successful management of rosacea involves a comprehensive approach customized to the patient's specific symptoms and disease severity. Topical therapies are typically the initial treatment choice, with agents like metronidazole, azelaic acid, and ivermectin proving effective in reducing inflammation and facial redness. For instance, a comprehensive review highlighted that these topical medications are effective in managing rosacea symptoms [26]. In cases where topical therapies are insufficient, systemic treatments may be employed. Oral antibiotics, particularly tetracyclines like doxycycline, are commonly prescribed due to their anti-inflammatory properties. A recent study noted that doxycycline is effective in reducing inflammatory lesions associated with rosacea. For patients presenting with persistent erythema, topical vasoconstrictive agents such as brimonidine and oxymetazoline can provide temporary relief by reducing facial redness. Additionally, laser and light-based therapies have emerged as valuable options, particularly for telangiectasia and refractory erythema. These modalities target vascular components of rosacea, leading to improved cosmetic outcomes. A recent review emphasized the importance of a phenotype-based approach to treatment, tailoring interventions to the individual's specific clinical features to optimize outcomes [27].

2.8 Alovera

Aloe vera (*Aloe barbadensis Miller*) is well known for its broad therapeutic benefits, especially in the fields of dermatology and wound care. The gel extracted from the plant contains bioactive compounds like acemannan, which possess anti-inflammatory, antimicrobial, and healing properties. These attributes make it beneficial in managing various skin conditions, including burns, cuts, and eczema.

2.9 Medical Plants

Medicinal plants are those that have shown therapeutic properties and have shown beneficial results on humans and animals. Medicinal plants have been used from early times for treatment of different diseases. In early times with their instincts, taste and smell ability humans used different plants. Some plants were directly applied to injuries, some were boiled to extract the components present in that plant for treatment. For this the therapeutic properties of many plants have been under consideration and these plants have been used as an important source for the lead drugs it has been integral to human healthcare for millennia, serving as foundational elements in traditional medicine systems and contributing significantly to modern pharmacology. Their therapeutic applications span a range of health conditions, like cancer, neurological disorders, cardiovascular disease, microbial infections, inflammation, and pain management [28]. The efficacy of medicinal plants is largely attributed to their diverse bioactive compounds, which have been the subject of extensive pharmacological studies. Its research has highlighted the immunomodulatory potential of certain plants, underscoring their role in enhancing immune responses.

2.10 Secondary Metabolities

Aloe vera (*Aloe barbadensis Miller*) is widely valued for its diverse range of secondary metabolites that play a crucial role in its therapeutic effects. Notably,

it contains anthraquinones like aloe-emodin, chrysophanol tricyclic aromatic compounds produced through a type III polyketide synthase pathway unique to plants. These molecules are well recognized for their potent anti-inflammatory and antimicrobial properties [29]. Another vital compound is aloesin, a C-glucosyl chromone that exhibits antioxidant and free radical scavenging properties, thereby enhancing the plant's therapeutic potential.

2.11 Pharmacological

Aloe vera (*Aloe barbadensis Miller*) exhibits a diverse range of pharmacological properties, making it a subject of extensive research in recent years. Notably, *Aloe vera* has shown effectiveness in lowering blood glucose levels, providing antioxidant and immune-regulating benefits, promoting apoptosis in cancer cells, safeguarding the liver from injury, and possessing antimicrobial activity [29]. Additionally, *Aloe vera*'s constituents have shown potential in preventing and treating various diseases, including their anti-inflammatory, anticancer, and antioxidant properties Furthermore, *Aloe vera*'s antiviral, antimicrobial, antitumor, and antifungal activities have been documented, highlighting its broad therapeutic applications [30]. The botanical classification of *Aloe vera* is detailed in Table 2.1, which outlines its full taxonomic hierarchy from kingdom to species level.

2.12 Taxonomic Hierarchy

Table 2.1: Taxonomic hierarchy of Alovera

Rank	**Classification**
Kingdom	Plantae
Clade	Angiosperms
Clade	Monocots
Order	Asparagales

continued on next page

Table 2.1 continued from previous page

Rank	**Classification**
Family	Asphodelaceae
Subfamily	Asphodeloideae
Genus	*Aloe*
Species	*Aloe vera*

2.13 Molecular Docking

Molecular docking is a computational method commonly employed to predict how a small molecule binds to a protein target, helping to elucidate molecular interactions and support drug discovery. Recent advancements have integrated machine learning with molecular docking to enhance predictive accuracy. For instance, a study curated a dataset of 2,640 Small-molecule inhibitors were designed to target jack bean urease, and a random forest classifier was developed, demonstrating high predictive performance. This approach, combined with physicochemical analyses and protein-ligand fingerprinting, provided deeper insights into the activity landscape of these inhibitors. To address challenges in analyzing extensive docking results, tools like InVADo have been developed. InVADo offers interactive visual analysis for large docking datasets through multiple linked 2D and 3D views, streamlining the evaluation process. Additionally, the reliability of selecting the top-scoring docking position as the best pose has been scrutinized. Research indicates that this selection is non-trivial, emphasizing the need for careful consideration beyond just energy scores [31, 32]. It plays a crucial role in structure-based virtual screening and hit-to-lead optimization, with its success largely relying on the precision of protein-ligand scoring functions. By estimating binding poses and affinities, molecular docking assists in identifying potential therapeutic compounds, thereby streamlining the drug development process. Moreover, advancements in docking methodologies have enhanced the assessment of antioxidant compounds, providing insights into their molecular interactions and potential health benefits [33, 35].

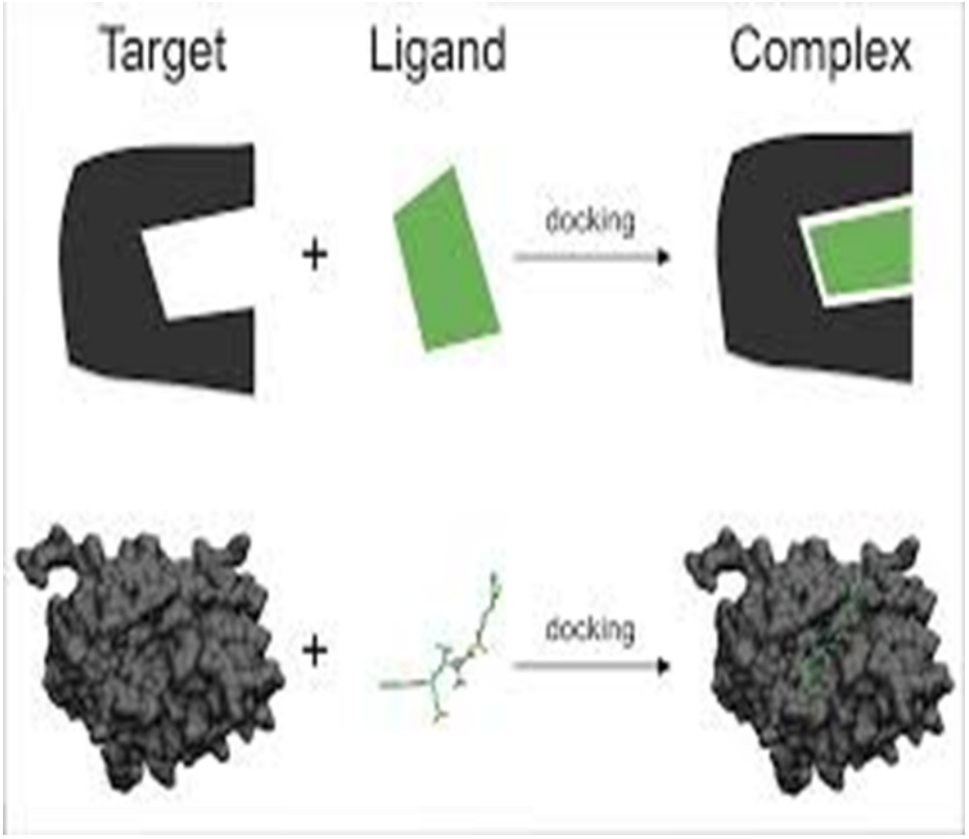

FIGURE 2.1: Docking [31]

2.14 Kallikrein 5 (KLK-5) Protease

KLK-5 is a serine protease that cleaves the inactive precursor hCAP18 into its active antimicrobial peptide form, LL-37, which plays a crucial role in immune responses and inflammation, particularly in conditions like rosacea. Cathelicidin, particularly its active form LL-37, is a vital component of human innate immune system, possessing broad-spectrum antimicrobial properties. The precursor protein, hCAP18, undergoes proteolytic cleavage to produce the active LL-37 peptide. This cleavage is primarily facilitated by the serine protease proteinase 3, which processes hCAP18 into LL-37.

Beyond proteinase 3, other proteases also interact with LL-37. For instance, Staphylococcus aureus produces aureolysin, a metalloproteinase that can degrade and inactivate LL-37, potentially aiding the bacterium in evading the host's immune response. Similarly, the cysteine protease ApdS from Streptococcus suis

cleaves LL-37, highlighting a mechanism by which certain pathogens might counteract the antimicrobial effects of LL-37 [36, 37].

The stability of LL-37 in various physiological environments is also influenced by proteolytic activity. In non-healing wounds, LL-37 can be degraded by serine proteases such as trypsin, which may impede the peptide's antimicrobial efficacy and contribute to persistent infections [38].

2.15 Natural Inhibitor

Kallikrein 5 (KLK-5) is a serine protease implicated in many kinds of skin conditions, including rosacea and atopic dermatitis, due to its role in processing antimicrobial peptides like cathelicidin (LL-37). Identifying natural compounds that inhibit KLK-5 offers potential therapeutic avenues. Triterpenoids is a compound Compounds such as ursolic acid and tumulosic acid have demonstrated inhibitory effects on KLK-5 activity. These triterpenoids suppressed KLK-5 protease activity and reduced the proteolytic processing of LL-37 in keratinocytes at concentrations $\leq$10 μM without cytotoxic effects. Additionally, these compounds were detectable in the plasma of rats administered with Jumihaidokuto, a triterpenoid-rich traditional medicine, suggesting potential systemic availability [39]. Isocoumarins is a Natural isocoumarins, including vioxanthin and 8,8'-paepalantine, have been identified as competitive inhibitors of KLK-5. Vioxanthin exhibited a Ki value of 22.9 μM against KLK-5.

Aloe vera has been recognized for its anti-inflammatory properties, which can help alleviate symptoms. *Aloe vera* contains bioactive compounds such as aloin, aloe-emodin, and acemannan, which contribute to its therapeutic effects. These compounds have been shown to reduce inflammation and promote skin healing, making *Aloe vera* a valuable component in managing rosacea symptoms. [41].

Furthermore, *Aloe vera*'s ability to enhance skin barrier function and provide antimicrobial effects adds to its potential benefits for individuals with rosacea. By

maintaining skin integrity and reducing microbial colonization, *Aloe vera* can help mitigate triggers that may exacerbate rosacea [42].

Chapter 3

Methodology

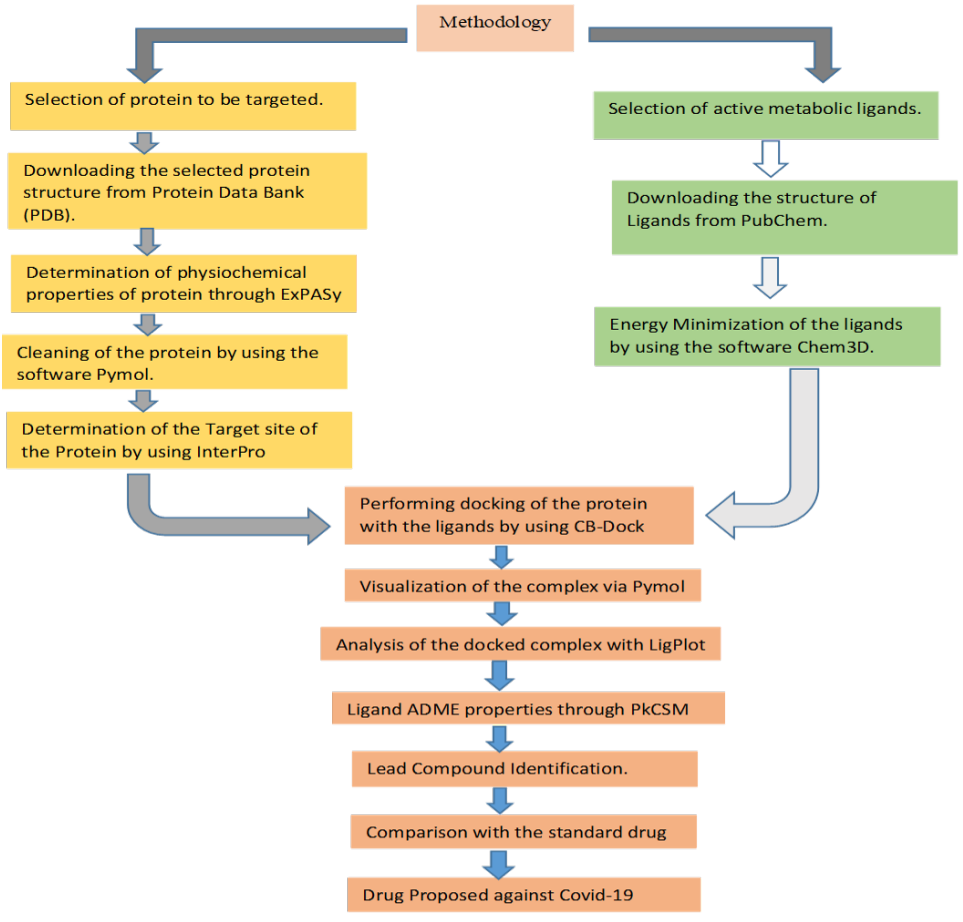

FIGURE 3.1: Overview of Methodology

3.1 Selection of Disease

Rosacea is a chronic inflammatory skin condition characterized by facial redness, pimples, and, in severe cases, thickened skin. A key factor in its pathogenesis is the overexpression of cathelicidin antimicrobial peptides, particularly LL-37, which, when processed by serine proteases like kallikrein 5 (KLK-5), lead to inflammatory responses. Targeting this pathway offers potential therapeutic avenues for managing rosacea symptoms [43].

3.2 Selection of Protein

Cathelicidin LL-37 played a pivotal role in inflammatory processes associated with rosacea. Its interaction with the NLRP3 inflammasome was implicated in promoting skin inflammation. Therefore, LL-37 was selected as a suitable target protein for *in silico* studies that aimed to identify potential inhibitors capable of mitigating rosacea symptoms [43].

3.3 Determination of Physiochemical Properties of Proteins

Understanding the physical and chemical properties of LL-37 was essential for elucidating its function and interactions. The ProtParam tool was used to analyze parameters such as molecular weight, isoelectric point, amino acid composition, and hydropathicity. This analysis was performed to provide insights into the peptide's behavior and stability [44].

3.4 Refining of the Downloaded Protein

After obtaining the 3D structure of LL-37 from protein databases, it was necessary to remove any non-essential molecules or artifacts. PyMOL software was used for

this purpose. The structure was cleaned to retain only the peptide chain required for subsequent analysis [45].

3.5 Determination of Functional Domains of Target Proteins

Identifying the functional domains of LL-37 was vital to understanding its mechanisms and interactions. The InterPro database was used for this analysis. This tool analyzed the peptide sequence to identify domains, families, and functional sites that could serve as potential binding regions for inhibitors [46].

3.6 Selection of Active Metabolic Ligands

Aloe vera (*Aloe barbadensis miller*) contained several bioactive compounds, including aloin, aloe-emodin, folic acid, and apigenin. These constituents demonstrated anti-inflammatory and antimicrobial properties, which made them suitable candidates for interaction studies with LL-37 [47].

3.7 Ligand Preparation

The 3D structures of *Aloe vera* constituents were obtained from databases like PubChem. In cases where the 3D structures were not available, canonical SMILES were used to generate the structures using ChemDraw. Energy minimization was then carried out using Chem3D Ultra. The prepared ligands were saved in appropriate formats, such as SDF, for molecular docking studies [48].

3.8 Molecular Docking

Molecular docking was performed to predict the binding affinity and orientation of the *Aloe vera* constituents with LL-37. The tool CB-Dock, which integrated AutoDock Vina, was used for this purpose. It automatically detected potential binding sites and conducted docking simulations. The results provided multiple binding poses and corresponding binding scores to help identify promising inhibitors [49].

3.9 Visualization of Docking Results via PyMOL

The docking interactions were visualized using PyMOL to examine the binding mechanisms. This tool allowed for the inspection of hydrogen bonds, hydrophobic interactions, and the overall fit of ligands within the binding pocket. The visualization helped interpret docking results and guided further optimization steps [50].

3.10 Analysis of Docked Complex via LigPlot

LigPlot was used to generate schematic diagrams illustrating protein–ligand interactions. These diagrams highlighted hydrogen bonds and hydrophobic contacts. This analysis helped assess the stability and specificity of the ligand–protein binding, which was essential in evaluating the compound's potential as an effective inhibitor [51].

3.11 Ligand ADME Properties

The ADME (Absorption, Distribution, Metabolism, and Excretion) properties of the selected compounds were analyzed using the pkCSM tool. This analysis was performed to evaluate the pharmacokinetic behavior of the ligands, thereby

identifying compounds with favorable profiles and excluding those with poor drug-like characteristics [52].

3.12 Lead Compound Identification

Lipinski's Rule of Five was applied to identify the most drug-like compound among the tested ligands. This rule included the following criteria:

- The log P value of the compound should be ≤ 5.
- The molecular weight should be less than 500 Da.
- The number of hydrogen bond acceptors should not exceed 10.
- The number of hydrogen bond donors should not exceed 5.

The compound that met all these parameters was selected as the lead compound. This step confirmed that the chosen compound possessed drug-like properties and warranted further development [53].

Chapter 4

Results and Discussions

4.1 Structure Modelling

Cathelicidin (*LL-37*) is selected as the target protein to act against the essential components present in Aloe vera *Aloe barbadensis Miller* [54]. The compounds include Fatty acids include *Hexadecenoic acid*, a common saturated fatty acid [55]. The anthraquinones group consists of *Aloe emodin* and *Chrysophanic acid*, both known for laxative as well as anti-inflammatory properties [56]. Polysaccharides include *Glucomannan* and *D-mannopyranose 6-phosphate*, which contribute to the immunomodulatory and moisturizing effects of aloe. Among the flavonoids, *Quercetin*, *Apigenin*, and *Kaempferol* are prominent for their antioxidant and anti-inflammatory activities [57]. The terpenes group is represented by *Aloesin*, *Isoaloeresin D*, *Aloeresin A*, *Cycloartenol*, and *Rosmarinic acid*, which are involved in skin protection, antimicrobial action, and pigmentation regulation. Steroids such as *Campesterol* and *Lupeol* play roles in anti-inflammatory and cholesterol-lowering effects [58]. Phenolic acids include *Ferulic acid*, *Caffeic acid*, *Gallic acid*, and *Salicylic acid*, all recognized for their strong antioxidant and anti-aging properties [59]. The vitamins category comprises Ascorbic acid (Vitamin C), Vitamin E acetate, and Folic acid, essential for skin health and cellular protection. Lastly, the saponins group includes *Aloesaponarin I* and *Aloesaponarin II*, known for their antimicrobial and cleansing properties [60].

4.1.1 3D Structure of the Protein

The 3D structure of cathelicidin (LL-37) from PDB ID 2K6O protein data bank DOI https://doi.org/10.2210/pdb2K6O/pdb as shown in Fig. 4.1.

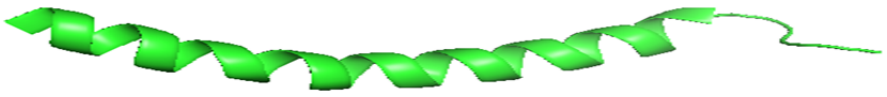

FIGURE 4.1: Structure of the protein

4.1.2 Physical Properties of Protein

To analyze the properties of the cathelicidin protein (LL-37), the ProtParam tool available on ExPASy is commonly used. This online tool calculates various physical and chemical characteristics of proteins, whether retrieved from databases like Swiss-Prot or TrEMBL, or directly entered by users [64]. The isoelectric point (pI) provides insight into the protein's charge properties: a pI above 7 indicates a basic protein, while a pI below 7 suggests an acidic nature [64]. The extinction coefficient reflects the protein's ability to absorb light, which is useful in protein quantification. The instability index helps predict protein stability *in vitro*; values below 40 suggest a stable protein, whereas values above 40 indicate that the protein may be unstable [64]. The detailed physical and chemical properties of cathelicidin (LL-37) are presented in Table 4.1.

TABLE 4.1: Physical properties of Cathelicidin(LL37)

MW	**pI**	**NR**	**PR**	**Ext. Co 2**	**Ext. Co 1**	**Instability index**	**Aliphatic index**	**GRAVY**
4493.32	10.61	5	11	0	0	23.34	89.46	-0.724

The aliphatic index indicates the thermo-stability of a protein, with higher values generally suggesting greater stability at elevated temperatures. The molecular

weight (MW) of the protein accounts for the total mass, including contributions from both positively and negatively charged amino acid residues. Specifically, NR represents the negatively charged residues (Aspartic acid + Glutamic acid), while PR denotes the positively charged residues (Arginine + Lysine). The GRAVY (Grand Average of Hydropathicity) value reflects the protein's hydrophilicity or hydrophobicity; lower GRAVY values indicate a stronger tendency to interact with water, suggesting higher solubility. All these parameters were carefully considered in the analysis of LL-37 [65].

4.1.3 Identification of Functional Domains of the Protein

For identifying the functional domains InterPro consortium is used. InterPro helps in finding the functional analysis of proteins and classifies them into families which is done by finding functional domains and other important sites. Functional domains are the active part of the protein that is used by the protein for interacting with other proteins or other substances [66].

4.1.4 Structure of Protein Refined for Docking

The structure of the protein is refined by the use of PyMol and then refined for docking.

4.2 Ligand Selection

The Protein Data Bank (PDB) contains extensive information on protein–ligand complexes. For this study, ligand selection was based on crystal structures with the best resolution, considering the chemical class of the ligand bound to the protein, as well as their binding affinities. An important factor in this process is the conformational selection of the ligand. This refers to the ligand's ability to bind preferentially to a specific protein conformation, thereby stabilizing it and increasing its relative abundance within the overall protein population [67].

The active compounds from the selected plant were identified using PubChem, the world's largest chemical database. The 3D structures of these ligands were downloaded in Structure Data File (SDF) format. The selected ligands, along with their molecular formulas, molecular weights, and structural details, are presented in Table 4.2.

Following the download, the next essential step was energy minimization of the ligand structures. This process is crucial because the raw downloaded structures are typically in a high-energy, unstable state. Using unrefined structures in molecular docking can negatively affect the accuracy of binding affinity predictions, such as Vina docking scores. Therefore, energy minimization ensures the ligands are in a stable, optimized form suitable for reliable docking simulations [68].

TABLE 4.2: List of Ligands with Molecular Formulas, Weights, and Structures

Sr. No.	**Name of Ligands**	**Molecular Formula**	**Molecular Weight**	**Structure**
1	Hexadecanoic acid	$C_{16}H_{32}O_2$	256.42 g/mol	
2	Aloin A	$C_{21}H_{22}O_9$	418.4 g/mol	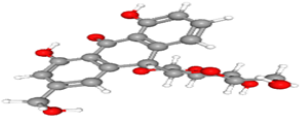
3	Aloe emodin	$C_{15}H_{10}O_5$	270.24 g/mol	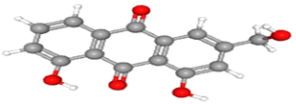
4	Chrysophanic acid	$C_{15}H_{10}O_4$	254.24 g/mol	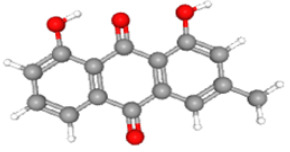
5	Glucomannan	$C_{24}H_{42}O_{21}$	666.6 g/mol	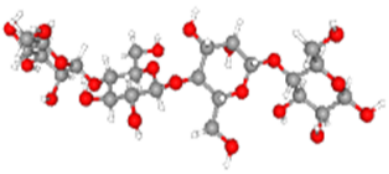

continued on next page

Sr. No.	Name of Ligands	Molecular Formula	Molecular Weight	Structure
6	D-mannopyranose 6-phosphate	$C_6H_{13}O_9P$	260.14 g/mol	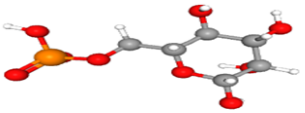
7	Aloesin	$C_{19}H_{22}O_9$	394.4 g/mol	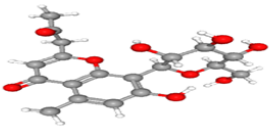
8	Isoaloeresin D	$C_{29}H_{32}O_{11}$	556.6 g/mol	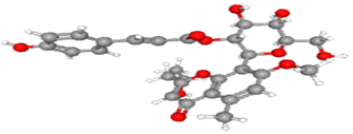
9	Aloeresin A	$C_{28}H_{28}O_{11}$	540.5 g/mol	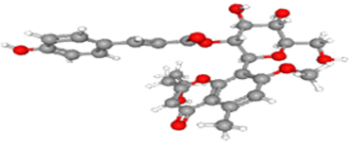
10	Campesterol	$C_{28}H_{48}O$	400.7 g/mol	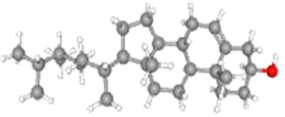
11	Lupeol	$C_{30}H_{50}O$	426.7 g/mol	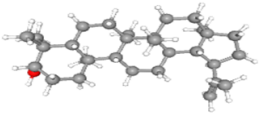
12	Salicylic Acid	$C_7H_6O_3$	138.12 g/mol	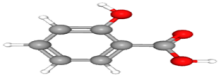
13	Caffeic acid	$C_9H_8O_4$	180.16 g/mol	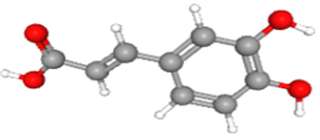
14	Ferulic acid	$C_{10}H_{10}O_4$	194.18 g/mol	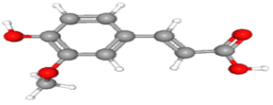

continued on next page

Sr. No.	Name of Ligands	Molecular Formula	Molecular Weight	Structure
15	Gallic acid	$C_7H_6O_5$	170.12 g/mol	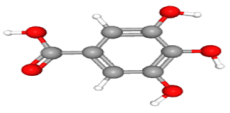
16	Kaempferol	$C_{15}H_{10}O_6$	286.24 g/mol	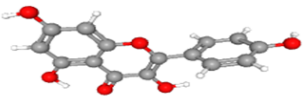
17	Quercetin	$C_{15}H_{10}O_7$	302.23 g/mol	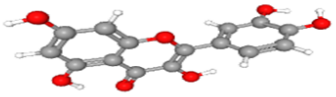
18	Apigenin	$C_{15}H_{10}O_5$	270.24 g/mol	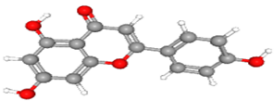
19	Cycloartenol	$C_{30}H_{50}O$	426.7 g/mol	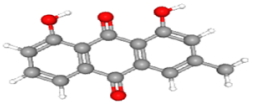
20	Ascorbic Acid	$C_6H_8O_6$	176.12 g/mol	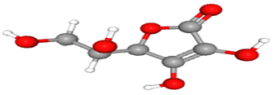
21	Vitamin E acetate	$C_{31}H_{52}O_3$	472.7 g/mol	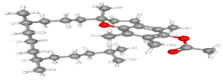
22	Folic Acid	$C_{19}H_{19}N_7O_6$	441.4 g/mol	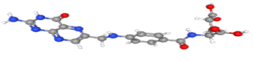
23	Aloesaponarin I	$C_{17}H_{12}O_6$	312.27 g/mol	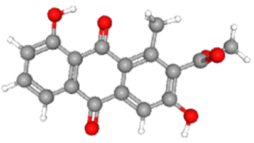
24	Aloesaponarin II	$C_{15}H_{10}O_4$	254.24 g/mol	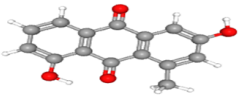

continued on next page

Sr. No.	Name of Ligands	Molecular Formula	Molecular Weight	Structure
25	Rosmarinic acid	$C_{18}H_{16}O_8$	360.3 g/mol	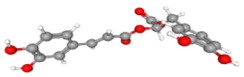

4.3 Virtual Screening and also its Toxicity Prediction through Lipinski Rule of Five

To differentiate between drug-like and non-drug-like compounds, the Lipinski Rule of Five and ADME (Absorption, Distribution, Metabolism, and Excretion) properties are commonly used. The Lipinski Rule of Five outlines key criteria for orally active drugs, which include: molecular weight $\leq$ 500 Da, log P (partition coefficient) $\leq$ 5, no more than 5 hydrogen bond donors, and no more than 10 hydrogen bond acceptors. These parameters help predict a compound's oral bioavailability [69]. The application of Lipinski's Rule to the selected ligands is summarized in Table 4.3, showing their log P values, molecular weights, and counts of hydrogen bond donors and acceptors.

The classification of a compound as drug-like also depends on its intended route of administration. Generally, a compound is considered drug-like if it satisfies at least three of the Lipinski rules. Conversely, if it violates two or more of these criteria, it is likely to have poor absorption and is considered non-drug-like [70].

TABLE 4.3: Application of Lipinski Rule on the Ligands

Sr. No.	Name	Log P Value	Molecular Weight	H-Bond Acceptor	H-Bond Donor
1	Hexadecanoic acid	5.5523	256.42 g/mol	1	1
2	Aloin A	-0.8912	418.4 g/mol	9	7

continued on next page

Table 4.3 continued from previous page

Sr. No.	Name	Log P Value	Molecular Weight	H-Bond Acceptor	H-Bond Donor
3	Aloe emodin	1.3655	270.24 g/mol	5	3
4	Chrysophanic acid	2.18162	254.24 g/mol	4	2
5	Glucomannan	-9.7488	666.6 g/mol	21	14
6	D-mannopyranose 6-phosphate	-3.1044	260.14 g/mol	7	6
7	Aloesin	-0.54658	394.4 g/mol	9	5
8	Isoaloeresin D	1.51812	556.6 g/mol	11	5
9	Aloeresin A	1.42332	540.5 g/mol	11	5
10	Campesterol	7.6347	400.7 g/mol	1	1
11	Lupeol	8.0248	426.7 g/mol	1	1
12	Salicylic Acid	1.0904	138.12 g/mol	2	2
13	Caffeic acid	1.1956	180.16 g/mol	3	3
14	Ferulic acid	1.4986	194.18 g/mol	3	2
15	Gallic Acid	0.5016	170.12 g/mol	4	4
16	Kaempferol	2.2824	286.24 g/mol	6	4
17	Quercetin	1.988	302.23 g/mol	7	5
18	Apigenin	2.5768	270.24 g/mol	5	3
19	Cycloartenol	8.1689	426.7 g/mol	1	1
20	Ascorbic Acid	-1.4074	176.12 g/mol	6	4
21	Vitamin E acetate	9.05996	472.7 g/mol	3	0
22	Folic Acid	-0.0448	441.4 g/mol	9	6
23	Aloesaponarin I	1.96822	312.27 g/mol	6	2
24	Aloesaponarin II	2.18162	254.24 g/mol	4	2
25	Rosmarinic acid	1.7613	360.3 g/mol	7	5

4.3.1 Toxicity Prediction

PkCSM is a web-based tool used to predict the ADMET (Absorption, Distribution, Metabolism, Excretion, and Toxicity) properties of bioactive compounds and drug

candidates. This tool enables the evaluation of the toxicity profiles of selected ligands through various predictive models [71].

One such model is the AMES toxicity test, which assesses the mutagenic potential of a compound using bacterial strains. A positive AMES result suggests that the compound may be mutagenic and potentially carcinogenic [72]. The *T. pyriformis* toxicity test evaluates the toxic effect of compounds on the protozoan Tetrahymena pyriformis. Toxicity is indicated when the predicted value exceeds -0.5 log μg/L [73].

The Minnow toxicity test estimates the concentration at which a compound may be lethal to 50% of the fathead minnows (LC−50). A value below 0.5 mM is considered acutely toxic.

The Maximum Recommended Tolerated Dose (MRTD) provides an estimate for the initial dosing level in Phase I clinical trials. A value of ≤ 0.477 log mg/kg/day is considered low, while values above this threshold are regarded as high [74].

The oral rat chronic toxicity test predicts the lowest observed adverse effect level (LOAEL) in rats, expressed in log mg/kg body weight per day. This value reflects the concentration at which adverse effects begin to appear during prolonged exposure [75].

Hepatotoxicity predictions help assess whether a compound is likely to cause liver damage, while skin sensitization predictions indicate the potential for dermatological reactions [76].

Finally, hERG I and II inhibitor tests predict the ability of a compound to block human ether-à-go-go-related gene (hERG) potassium channels. Inhibition of these channels may prolong the QT interval, potentially leading to QT syndrome and, over time, life-threatening arrhythmias such as ventricular tachycardia or fibrillation [77, 78]. Detailed toxicity results for all 25 ligands are summarized in Tables 4.4 to 4.11, grouped based on compound sets. These tables offer a comprehensive overview of predicted toxicological parameters, supporting compound prioritization for further drug development studies.

4.3.1.1 Hexadecanoic Acid, Aloin A and Aloe emodin

TABLE 4.4: Application of Lipinski Rule on the Ligands

S. No.	Model Name	Predicted Value of Hexadecanoic acid	Predicted Value of Aloin A	Predicted Value of Aloe emodin
1	AMES Mutagenicity Test	-	-	+
2	Maximum Tolerated Dose in Humans (log mg/kg/-day)	-0.708	0.425	-0.089
3	hERG Channel Blocker – Type I	-	-	-
4	hERG Channel Blocker – Type II	-	-	-
5	Acute Oral Toxicity in Rats (LD_{50}, log mol/kg)	1.44	2.712	2.329
6	Chronic Oral Toxicity in Rats (LOAEL, log mg/kg bw/day)	3.181	3.316	1.878
7	Liver Toxicity Potential (Hepatotoxicity)	-	-	-
8	Potential for Skin Allergy (Sensitization)	+	-	-
9	*T. pyriformis* Toxicity (log μg/L)	0.84	0.285	0.563
10	Minnow Toxicity – LC_{50} (log mM)	-1.083	6.437	2.337

In this table "+" indicates Yes and "-" indicates No.

4.3.1.2 Chrysophanic Acid Glucomannan & D - mannopyranose 6 - phosphate

Table 4.5 shows that Chrysophanic acid is mutagenic in the AMES test, while Glucomannan and D-mannopyranose 6-phosphate are not.

None of the compounds show hepatotoxicity or skin sensitization. Glucomannan has the highest tolerated dose and lowest acute/chronic toxicity, but it is a potential hERG II blocker.

Overall, Glucomannan and D-mannopyranose 6-phosphate exhibit safer toxicity profiles than Chrysophanic acid.

TABLE 4.5: Toxicity values of Chrysophanic Acid, Glucomannan and D - mannopyranose 6 - phosphate

S. No	**Model Name**	**Predicted Value of Chrysophanic acid**	**Predicted Value of Glucomannan**	**Predicted Value of D-mannopyranose 6-phosphate**
1	AMES Mutagenicity Test	+	-	-
2	Maximum Tolerated Dose in Humans (log mg/kg/-day)	-0.256	0.367	1.577
3	hERG Channel Blocker – Type I	-	-	-
4	hERG Channel Blocker – Type II	-	+	-
5	Acute Oral Toxicity in Rats (LD_{50}, log mol/kg)	2.275	2.449	1.709
6	Chronic Oral Toxicity in Rats (LOAEL, log mg/kg bw/day)	2.057	5.477	4.289
7	Liver Toxicity Potential (Hepatotoxicity)	-	-	-
8	Potential for Skin Allergy (Sensitization)	-	-	-
9	*T. pyriformis* Toxicity (log μg/L)	0.794	0.285	0.285
10	Minnow Toxicity – LC_{50} (log mM)	1.603	21.017	6.463

In this table "+" indicates Yes and "-" indicates No.

4.3.1.3 Aloesin, Isoaloeresin D and Aloeresin A

Table 4.6 shows that none of the compounds are mutagenic or skin sensitizers.

However, all are predicted to be hepatotoxic, and both Isoaloeresin D and Aloeresin A are hERG II blockers. Their toxicity values are moderate overall, with Aloesin having the highest tolerated dose.

TABLE 4.6: Toxicity values of Aloesin Isoaloeresin D and Aloeresin A

S. No	**Model Name**	**Predicted Value of Aloesin**	**Predicted Value of Isoaloeresin D**	**Predicted Value of Aloeresin A**
1	AMES Mutagenicity Test	-	-	-
2	Maximum Tolerated Dose in Humans (log mg/kg/-day)	0.437	0.012	0.006
3	hERG Channel Blocker – Type I	-	-	-
4	hERG Channel Blocker – Type II	+	+	+
5	Acute Oral Toxicity in Rats (LD_{50}, log mol/kg)	2.47	2.645	2.621
6	Chronic Oral Toxicity in Rats (LOAEL, log mg/kg bw/day)	3.95	3.773	3.663
7	Liver Toxicity Potential (Hepatotoxicity)	+	+	+
8	Potential for Skin Allergy (Sensitization)	-	-	-
9	*T. pyriformis* Toxicity (log μg/L)	0.285	0.286	0.286
10	Minnow Toxicity – LC_{50} (log mM)	4.394	3.361	2.714

In this table "+" indicates Yes and "-" indicates No.

4.3.1.4 Campesterol, Lupeol, Salicylic Acid

Table 4.7 indicates all compounds are non-mutagenic, non-hepatotoxic, and non-sensitizers.

Campesterol and Lupeol show hERG II blocking activity. Salicylic acid has the highest tolerated dose and lowest chronic toxicity risk.

TABLE 4.7: Toxicity values of Campesterol, Lupeol ,Salicylic Acid

S. No	**Model Name**	**Predicted Value of Campesterol**	**Predicted Value of Lupeol**	**Predicted Value of Salicylic Acid**
1	AMES Mutagenicity Test	-	-	-
2	Maximum Tolerated Dose in Humans (log mg/kg/day)	-0.641	-0.502	0.61
3	hERG Channel Blocker – Type I	-	-	-
4	hERG Channel Blocker – Type II	+	+	-
5	Acute Oral Toxicity in Rats (LD_{50}, log mol/kg)	2.28	2.563	2.282
6	Chronic Oral Toxicity in Rats (LOAEL, log mg/kg bw/day)	0.867	0.89	2.483
7	Liver Toxicity Potential (Hepatotoxicity)	-	-	-
8	Potential for Skin Allergy (Sensitization)	-	-	-
9	*T. pyriformis* Toxicity (log μg/L)	0.513	0.316	0.263
10	Minnow Toxicity – LC_{50} (log mM)	-1.807	-1.696	1.812

In this table "+" indicates Yes and "-" indicates No.

4.3.1.5 Caffeic Acid Ferulic Acid Gallic Acid

Table 4.8 reveals all three compounds are safe in terms of mutagenicity, hepatotoxicity, and hERG inhibition. Gallic acid shows the lowest acute toxicity, while Caffeic acid has the highest tolerated dose.

TABLE 4.8: Toxicity values of Caffeic Acid Ferulic Acid Gallic Acid

S. No	**Model Name**	**Predicted Value of Caffeic acid**	**Predicted Value of Ferulic acid**	**Predicted Value of Gallic Acid**
1	AMES Mutagenicity Test	-	-	-
2	Maximum Tolerated Dose in Humans (log mg/kg/day)	1.145	1.082	0.7
3	hERG Channel Blocker – Type I	-	-	-
4	hERG Channel Blocker – Type II	-	-	-
5	Acute Oral Toxicity in Rats (LD_{50}, log mol/kg)	2.383	2.282	2.218
6	Chronic Oral Toxicity in Rats (LOAEL, log mg/kg bw/day)	2.092	2.065	3.06
7	Liver Toxicity Potential (Hepatotoxicity)	-	-	-
8	Potential for Skin Allergy (Sensitization)	-	-	-
9	*T. pyriformis* Toxicity (log μg/L)	0.293	0.271	0.285
10	Minnow Toxicity – LC_{50} (log mM)	2.246	1.825	3.188

In this table "+" indicates Yes and "-" indicates No.

4.3.1.6 Kaempferol Quercetin Apigenin

Table 4.9 reports no toxicity alerts for any of the three flavonoids. All are non-mutagenic, non-hepatotoxic, and safe for the heart and skin. Kaempferol shows the highest tolerated dose among them.

TABLE 4.9: Toxicity values of Kaempferol Quercetin Apigenin

S. No	**Model Name**	**Predicted Value of Kaempferol**	**Predicted Value of Quercetin**	**Predicted Value of Apigenin**
1	AMES Mutagenicity Test	-	-	-
2	Maximum Tolerated Dose in Humans (log mg/kg/day)	0.531	0.499	0.328
3	hERG Channel Blocker – Type I	-	-	-
4	hERG Channel Blocker – Type II	-	-	-
5	Acute Oral Toxicity in Rats (LD_{50}, log mol/kg)	2.449	2.471	2.45
6	Chronic Oral Toxicity in Rats (LOAEL, log mg/kg bw/day)	2.505	2.612	2.298
7	Liver Toxicity Potential (Hepatotoxicity)	-	-	-
8	Potential for Skin Allergy (Sensitization)	-	-	-
9	*T. pyriformis* Toxicity (log μg/L)	0.312	0.288	0.38
10	Minnow Toxicity – LC_{50} (log mM)	2.885	3.721	2.432

In this table "+" indicates Yes and "-" indicates No.

4.3.1.7 Cycloartenol Ascorbic Acid Vitamin E acetate

Table 4.10 indicates that all three compounds are generally non-toxic. Cycloartenol and Vitamin E acetate are predicted hERG II blockers, but no hepatotoxicity or skin sensitization is observed. Ascorbic acid shows the highest tolerated dose.

TABLE 4.10: Toxicity values of Cycloartenol Ascorbic Acid Vitamin E Acetate

S. No	**Model Name**	**Predicted Value of Cycloartenol**	**Predicted Value of Ascorbic Acid**	**Predicted Value of Vitamin E acetate**
1	AMES Mutagenicity Test	-	-	-
2	Maximum Tolerated Dose in Humans (log mg/kg/day)	-0.46	1.598	0.645
3	hERG Channel Blocker – Type I	-	-	-
4	hERG Channel Blocker – Type II	+	-	+
5	Acute Oral Toxicity in Rats (LD_{50}, log mol/kg)	2.627	1.063	1.908
6	Chronic Oral Toxicity in Rats (LOAEL, log mg/kg bw/day)	0.806	3.186	2.682
7	Liver Toxicity Potential (Hepatotoxicity)	-	-	-
8	Potential for Skin Allergy (Sensitization)	-	-	-
9	*T. pyriformis* Toxicity (log μg/L)	0.305	0.285	0.786
10	Minnow Toxicity – LC_{50} (log mM)	-1.928	4.386	-4.045

In this table "+" indicates Yes and "-" indicates No.

4.3.1.8 Folic Acid Aloesaponarin I Rosmarinic acid

Table 4.11 shows Aloesaponarin I and II are mutagenic, while Folic Acid and Rosmarinic acid are not. Only Folic Acid is hepatotoxic. All compounds are non-sensitizers and non-cardiotoxic. Rosmarinic acid has the highest tolerated dose and lowest aquatic toxicity.

TABLE 4.11: Toxicity values of Folic Acid, Aloesaponarin I, Rosmarinic Acid

Sr.	**Model Name**	**Predicted Value of Folic Acid**	**Predicted Value of Aloe-saponarin I**	**Predicted Value of Aloe-saponarin II**	**Predicted Value of Rosmarinic acid**
1	AMES Mutagenicity Test	-	+	+	+
2	Maximum Tolerated Dose in Humans (log mg/kg/day)	-0.586	0.147	0.51	0.152
3	hERG Channel Blocker – Type I	-	-	-	-
4	hERG Channel Blocker – Type II	-	-	-	-
5	Acute Oral Toxicity in Rats (LD_{50}, log mol/kg)	2.67	1.766	2.162	2.811
6	Chronic Oral Toxicity in Rats (LOAEL, log mg/kg bw/day)	3.153	1.821	2.211	2.907
7	Liver Toxicity Potential (Hepatotoxicity)	+	-	-	-

continued on next page

Table 4.11 continued from previous page

Sr.	Model Name	Predicted Value of Folic Acid	Predicted Value of Aloe-saponarin I	Predicted Value of Aloe-saponarin II	Predicted Value of Rosmarinic acid
8	Potential for Skin Allergy (Sensitization)	-	-	-	-
9	*T. pyriformis* Toxicity (log μg/L)	0.285	0.486	0.708	0.302
10	Minnow Toxicity – LC_{50} (log mM)	4.009	1.502	1.337	2.698

In this table "+" indicates Yes and "-" indicates No

4.4 Molecular Docking

Molecular docking is employed to estimate the binding affinity between a ligand and a receptor protein using the Vina scoring function, as well as to predict the optimal ligand conformation within the protein's binding site. This process requires the 3D structures of both the protein and ligands. In this study, CB-Dock, an online blind docking tool, was utilized for the docking procedure [79].

CB-Dock identifies potential binding pockets on the protein, calculates cavity sizes, and conducts docking using the widely-used Auto Dock Vina program. It generates five top-ranked binding poses along with corresponding receptor-ligand models. The best pose is then selected based on the Vina score and cavity size [79, 80].

For this analysis, Cathalidine was used as the receptor protein, while 25 selected ligands were docked as shown in Fig 4.12. The protein structure was obtained in PDB format, and the ligands were prepared in SDF format. CB-Dock verifies the

input files and converts them into the required PDBQT format using Open Babel and MGL Tools [81].

CB-Dock identifies the receptor's cavities and calculates the centers and sizes of the top five binding pockets. From these, the best conformation is chosen based on the highest affinity score indicating the strength of interaction between the protein and the ligand. Ligands exhibiting the strongest binding scores with the protein are considered the most promising [82]. A complete summary of the docking results, including all these parameters for each ligand, is presented in Table 4.12.

TABLE 4.12: Molecular docking

Sr. No.	**Name**	**Binding Score**	**Cavity Size**	**Log P Value**	**Molecular Weight**	**HBA**	**HBD**
1	Hexadecanoic acid	-4.1	19	5.5523	256.42 g/mol	1	1
2	Aloin A	-5.5	19	-0.8912	418.4 g/mol	9	7
3	Aloe emodin	-5.5	19	1.3655	270.24 g/mol	5	3
4	Chrysophanic acid	-4.9	19	2.18162	254.24 g/mol	4	2
5	Glucomannan	-5	19	-9.7488	666.6 g/mol	21	14
6	D-mannopyranose 6-phosphate	-4.4	12	-3.1044	260.14 g/mol	7	6
7	Aloesin	-5.8	19	-0.54658	394.4 g/mol	9	5
8	Isoaloeresin D	-6.6	19	1.51812	556.6 g/mol	11	5
9	Aloeresin A	-5.6	19	1.42332	540.5 g/mol	11	5
10	Campesterol	-5.8	10	7.6347	400.7 g/mol	1	1
11	Lupeol	-5.9	10	8.0248	426.7 g/mol	1	1
12	Salicylic Acid	-3.9	19	1.0904	138.12 g/mol	2	2
13	Caffeic acid	-4.1	8	1.1956	180.16 g/mol	3	3
14	Ferulic acid	-4.3	19	1.4986	194.18 g/mol	3	2
15	Gallic Acid	-3.9	19	0.5016	170.12 g/mol	4	4
16	Kaempferol	-5.1	19	2.2824	286.24 g/mol	6	4

continued on next page

Table 4.12 continued from previous page

Sr. No.	Name	Binding Score	Cavity Size	Log P Value	Molecular Weight	HBA	HBD
17	Quercetin	-5.1	19	1.988	302.23 g/mol	7	5
18	Apigenin	-5.1	19	2.5768	270.24 g/mol	5	3
19	Cycloartenol	-5.9	10	8.1689	426.7 g/mol	1	1
20	Ascorbic Acid	-3.8	19	-1.4074	176.12 g/mol	6	4
21	Vitamin E acetate	-6.2	19	9.05996	472.7 g/mol	3	0
22	Folic Acid	-6.3	5	-0.0448	441.4 g/mol	9	6
23	Aloesaponarin I	-5	19	1.96822	312.27 g/mol	6	2
24	Aloesaponarin II	-5.1	19	2.18162	254.24 g/mol	4	2
25	Rosmarinic acid	-5.8	19	1.7613	360.3 g/mol	7	5

4.5 Interaction of Ligands and the Targeted Protein

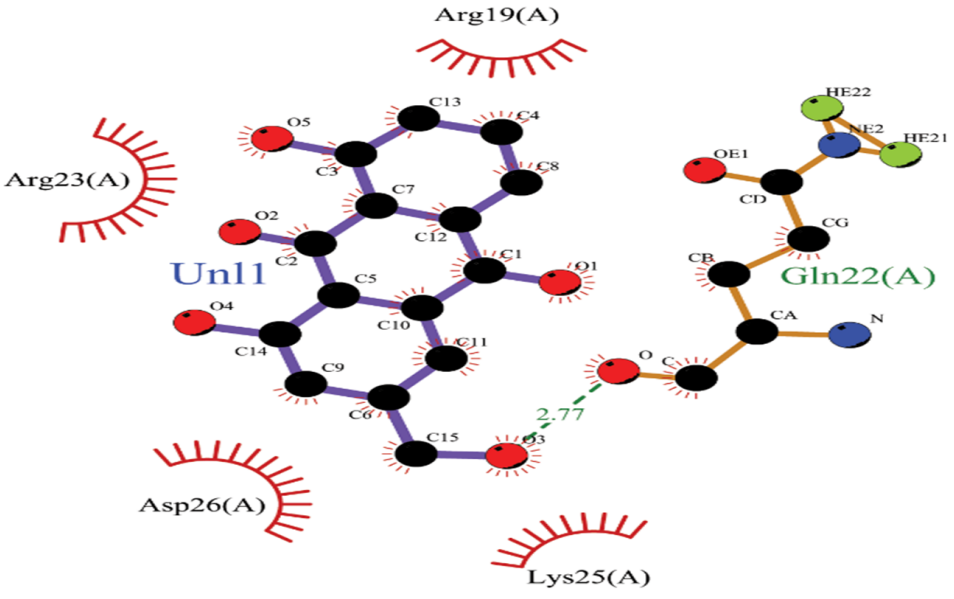

FIGURE 4.2: Interaction of Aloeemodin with receptor protein

2D interaction diagram of Aloeeemodin with the target protein. It forms one hydrogen bond with Gln22(A) Distance (2.77 Å) and interacts hydrophobically with Arg19(A), Arg23(A), Lys25(A), and Asp26(A), indicating a stable binding orientation.

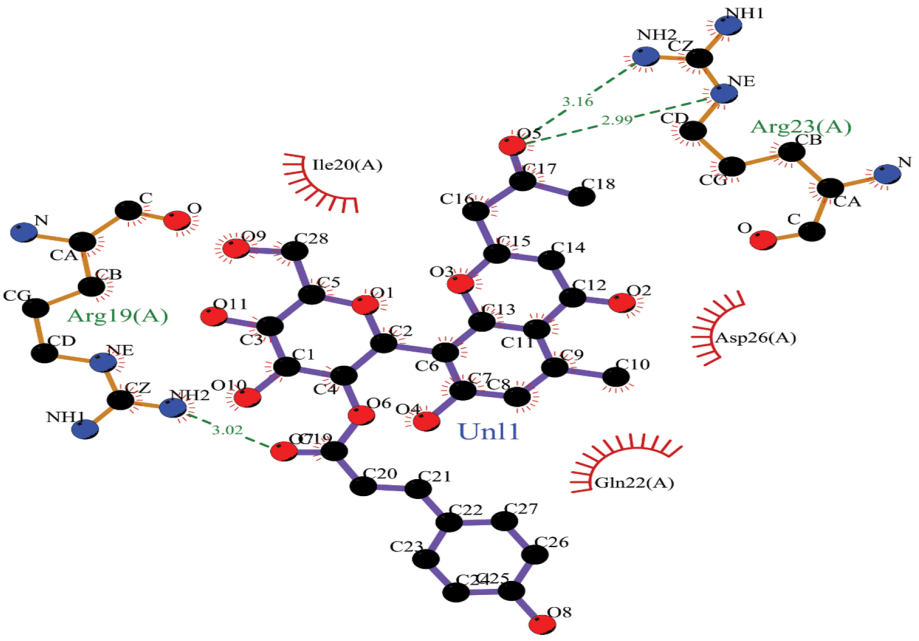

FIGURE 4.3: Interaction of Aloeresin A with the receptor protein

2D interaction diagram of Aloeresin A (Unl1) docked with the target protein. Aloeresin A forms two hydrogen bonds with Arg23(A) at distances of 2.98 Åand 3.16 Å, and shows hydrophobic interactions with Arg19(A), Ile20(A), Asp26(A), and Gln22(A), indicating stable binding within the active site.

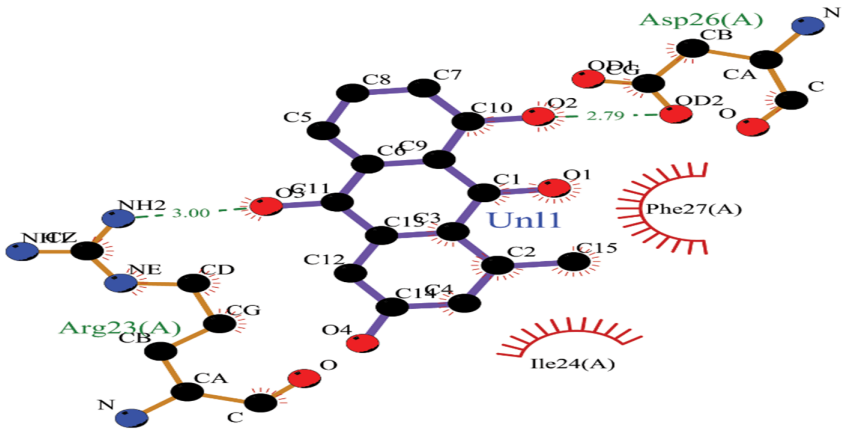

FIGURE 4.4: Interaction of Aloesaponarin II with the receptor protein

2D interaction diagram aloesaponarinII of with the target protein. It forms two hydrogen bond one with Arg23(A) Distance (3.00 Å) one other with Asp26(A) Distance (2.79 Å) and interacts hydrophobically with Phe27(A), Ile24(A), indicating a stable binding orientation.

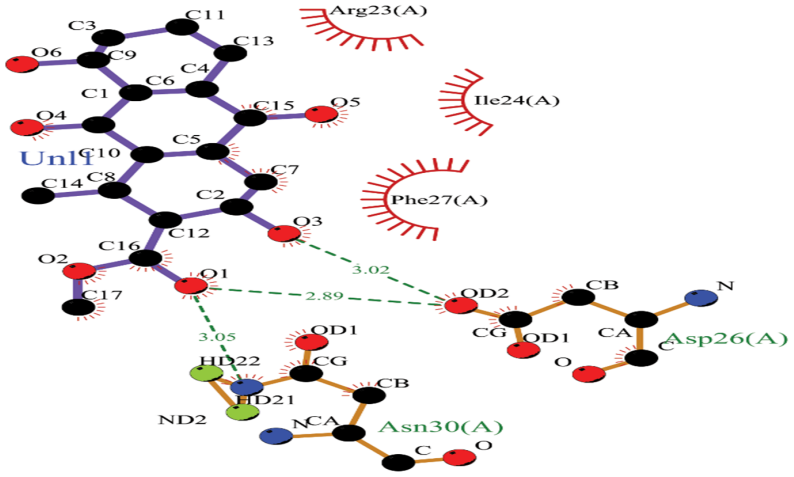

FIGURE 4.5: Interaction of Aloesaponarin I with the receptor protein

2D interaction diagram of Aloesaponarin I (Unl1) docked with the target protein. Aloesaponarin I forms three hydrogen bonds with Asp26(A) (2.89, 3.00 Å) and Asn30(A) (3.03 Å). Hydrophobic interactions are observed with Arg23(A), Ile24(A), and Phe27(A), suggesting strong and stable ligand binding.

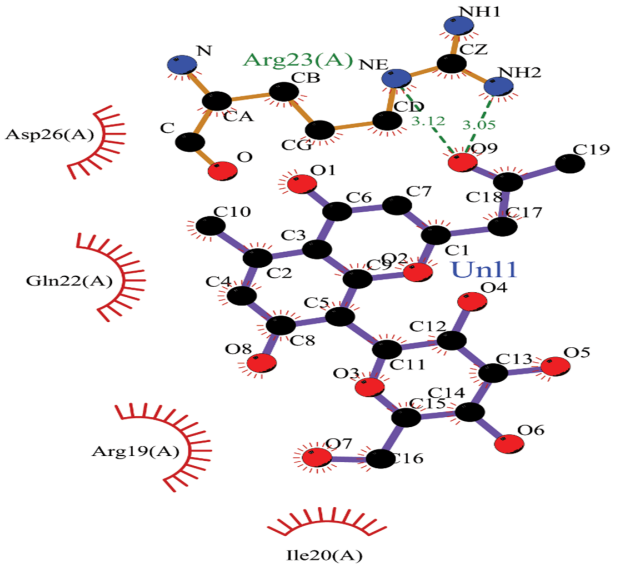

FIGURE 4.6: Interaction of aloesin with the receptor protein

2D interaction diagram of Alosin (Unl1) docked with the target protein. Aloeresin A forms two hydrogen bonds with Arg23(A) at distances of 3.03 Åand 3.14 Å, and shows hydrophobic interactions with Asp26(A), Ile20(A),Gln22 (A), and Arg19(A), indicating stable binding within the active site.

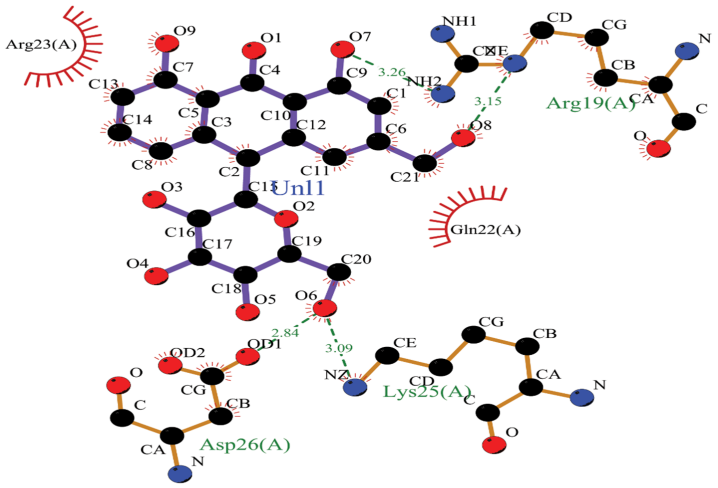

FIGURE 4.7: Interaction of AloinA with the receptor protein

Aloin A shows hydrophobic interactions with Arg23, Gln 22 it forms two bonds on Arg19 at distance of 3.26 and 3.13 and one bond on Lys25 at distance of 3.09 and Asp26 at distance of 2.83.

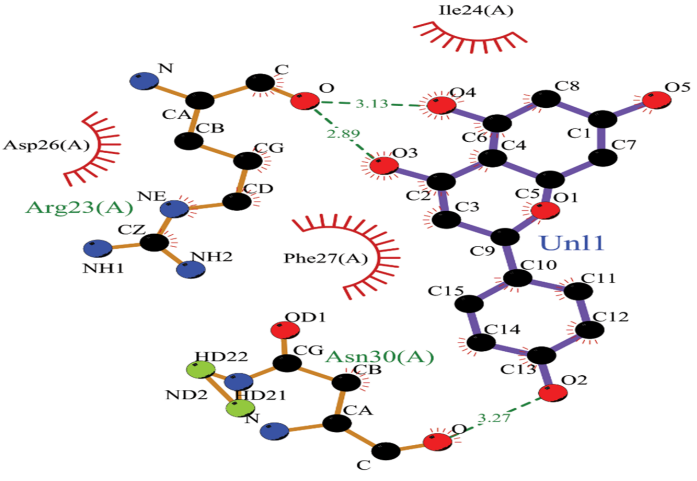

FIGURE 4.8: Interaction of Apigenin with the receptor protein

Apigenin shows hydrophobic interactions with Asp26, Ile24,Phe27. It forms bond with Asn30 at distance of 3.27 and Arg 23 at distance of 2.89 and 3.14.

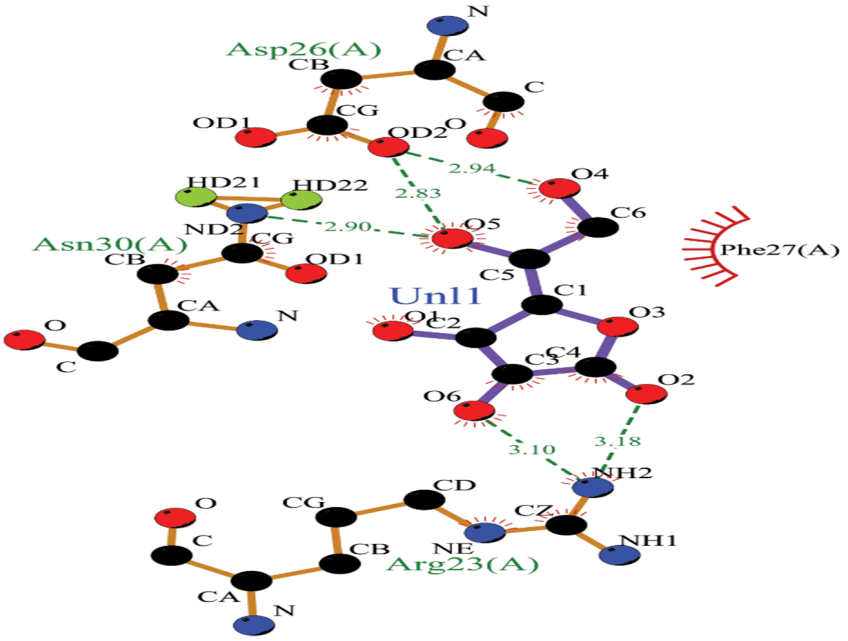

FIGURE 4.9: Interaction of Ascorbic Acid with the receptor protein

AscorbicAcid shows hydrophobic interactions with Phe27and forms bond with Arg23 at distance of 3.11 and 3.09 and Asn30 at distance of 2.92 and Asp26 at distance of 2.79 and 2.95.

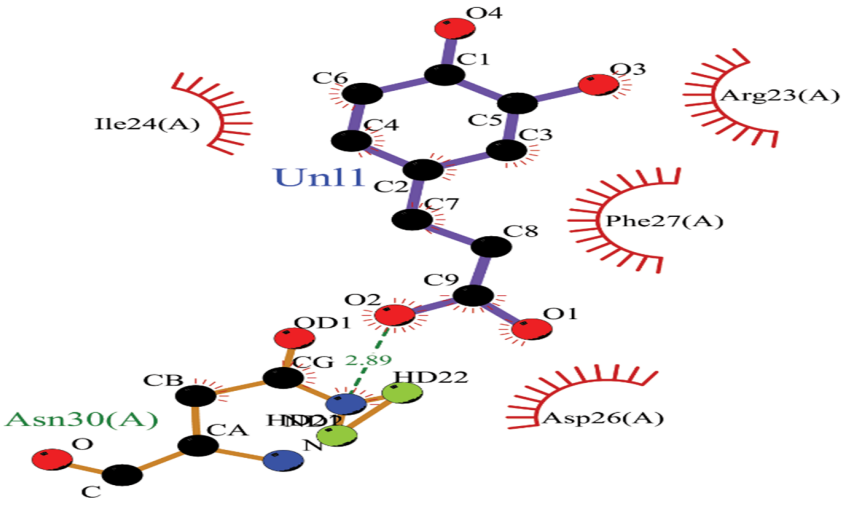

FIGURE 4.10: Interaction of Caffeic Acid with the receptor protein

CaffeicAcid shows hydrophobic interactions with Phe27,Arg23,Ile24 and forms bond with Asn30 at distance of 2.89 and Asp26 at distance of 2.88 and 3.06.

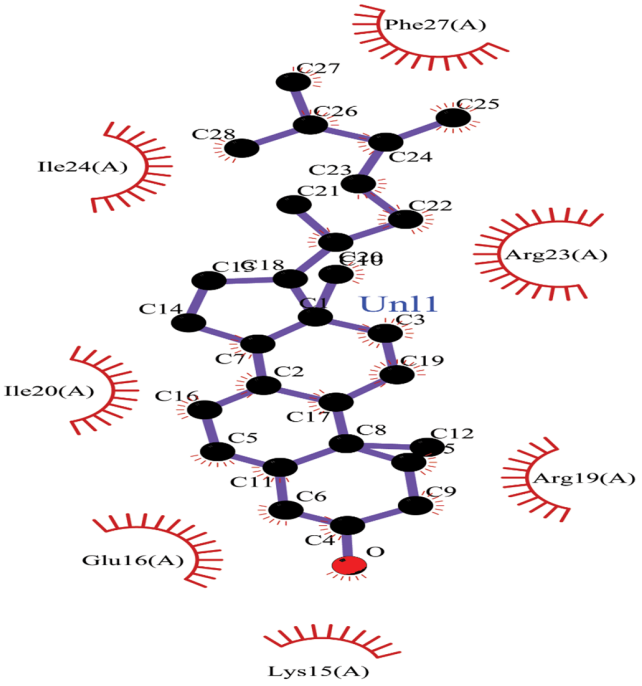

FIGURE 4.11: Interaction of Campesterol with the receptor protein

Campesterol shows hydrophobic interactions with Asp26,Arg23,Phe27,Ile24 it forms bond with Asn 30 at Distance of 3.13.

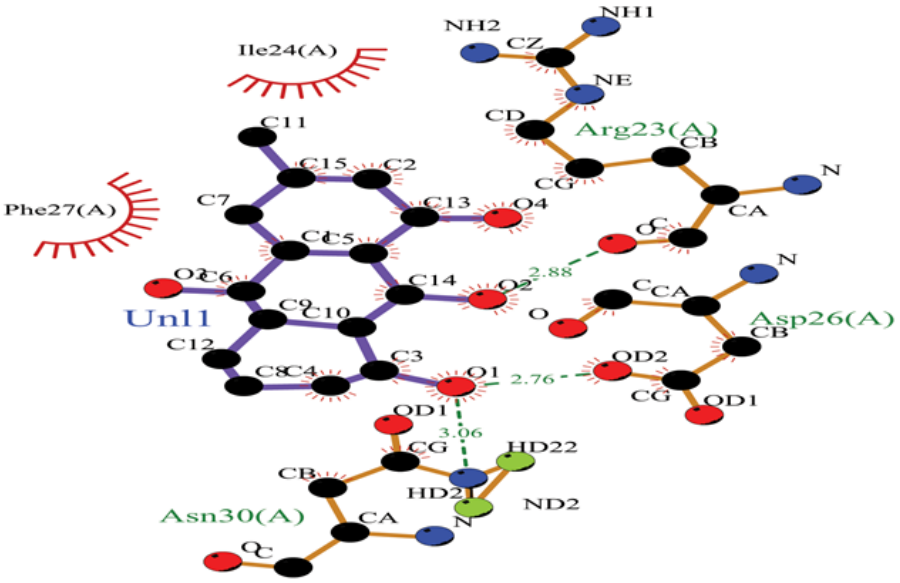

FIGURE 4.12: Interaction of Chrysophanic Acid with the receptor protein

Chrysophanic acid shows hydrophobic interactions with Asp26, Phe27. It forms bond with Asn30 at distance of 3.06 and with Arg23 at 2.87.

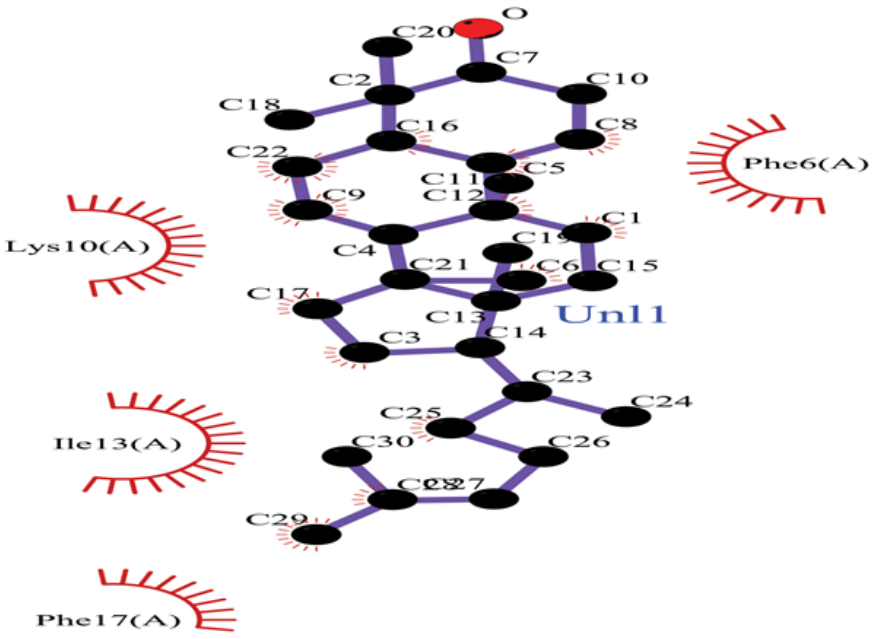

FIGURE 4.13: Interaction of Cycloartenol with the receptor protein

Cycloartenol shows hydrophobic interactions with Phe6, Lys10, Ile13, Phe17.

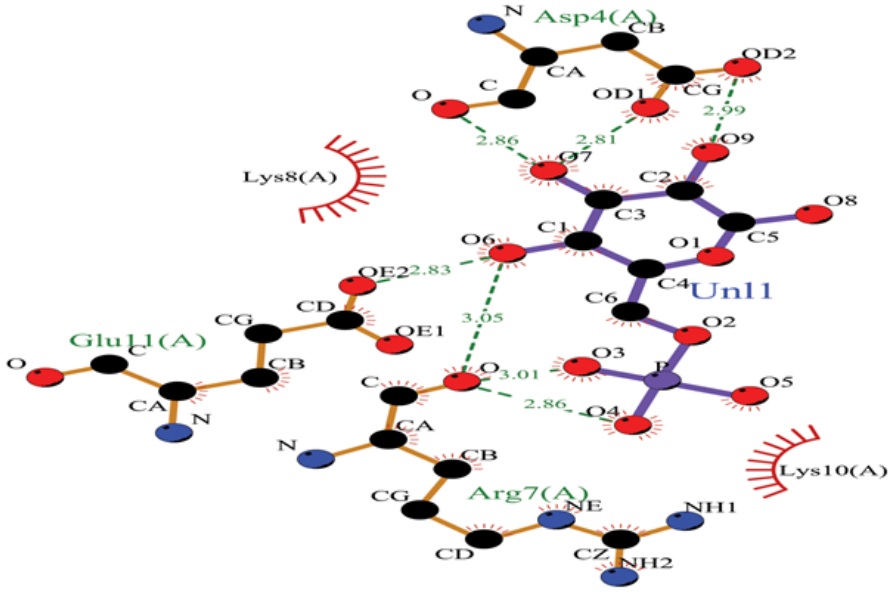

FIGURE 4.14: Interaction of D-mannopyranose 6-phosphate with the receptor protein

D-mannopyranose6-phosphate shows hydrophobic interactions with Lyz8, Lyz10 and forms bond with Glu, Arg and Asp 4.

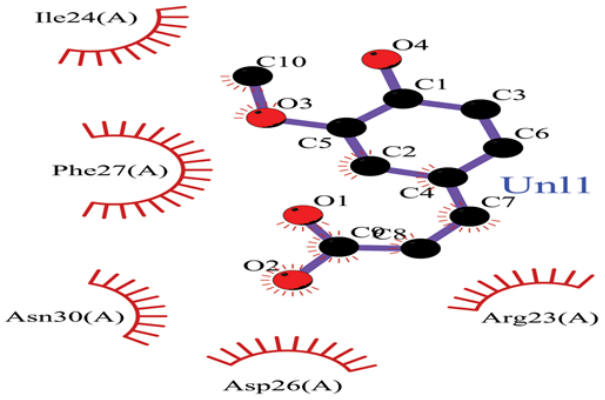

FIGURE 4.15: Interaction of Ferulic Acid with the receptor protein

Ferulic acid shows hydrophobic interactions with Arg23, Asp26, Asn30, Phe27, Ile24.

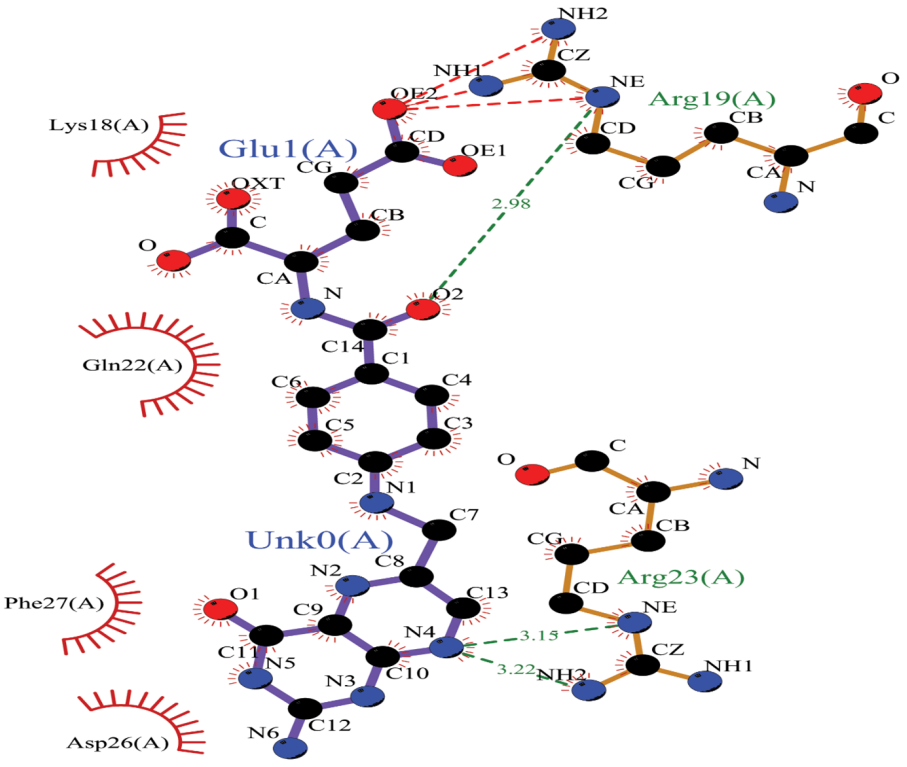

FIGURE 4.16: Interaction of Folic Acid with the receptor protein

Folic Acid interacts with Arg23(A), Glu22(A), Arg19(A) it forms bond with Asp26, Arg19, Arg23.

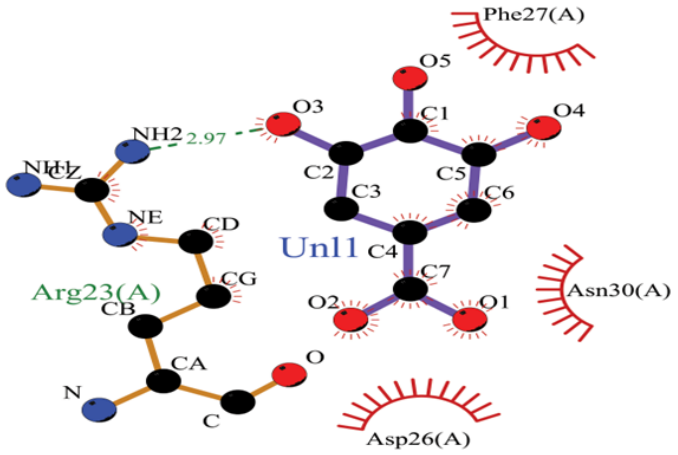

FIGURE 4.17: Interaction of Gallic Acid with the receptor protein

Gallic Acid shows hydrophobic interactions with Phe27, Asn30, Asp26 and forms bond between Arg23 at 2.97.

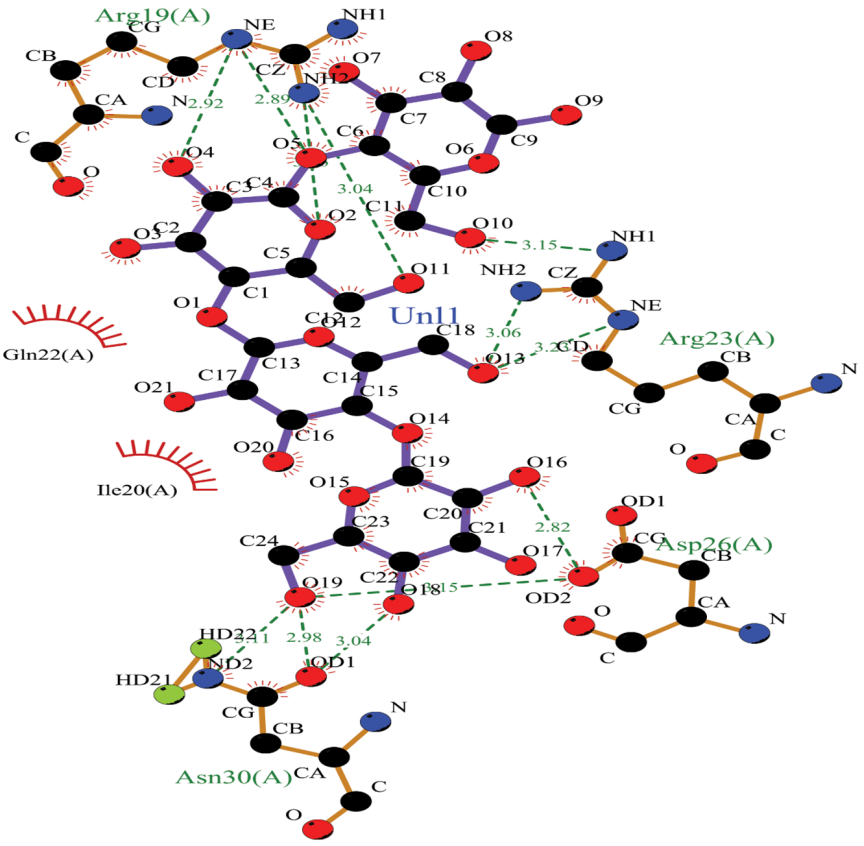

FIGURE 4.18: Interaction of Glucomannan with the receptor protein

Glucomannan shows hydrophobic interactions with Ile20 and forms different bonds at different points.

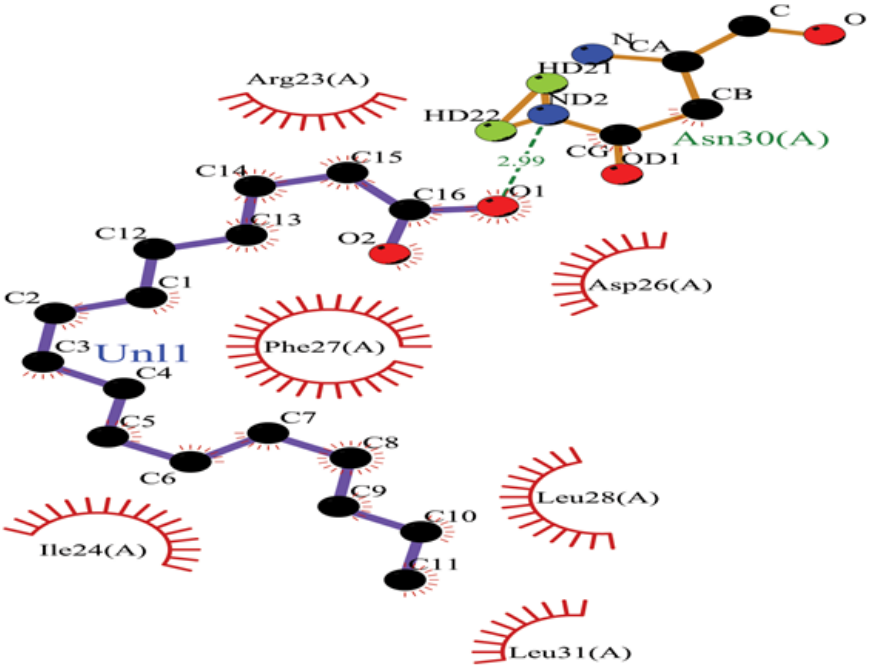

FIGURE 4.19: Interaction of Hexadecanoic Acid with the receptor protein

Hexadecenoic shows hydrophobic interactions with Ile20, Ile24, Arg23, Asp26, Phe27 and forms bond with Asn30 at 2.95.

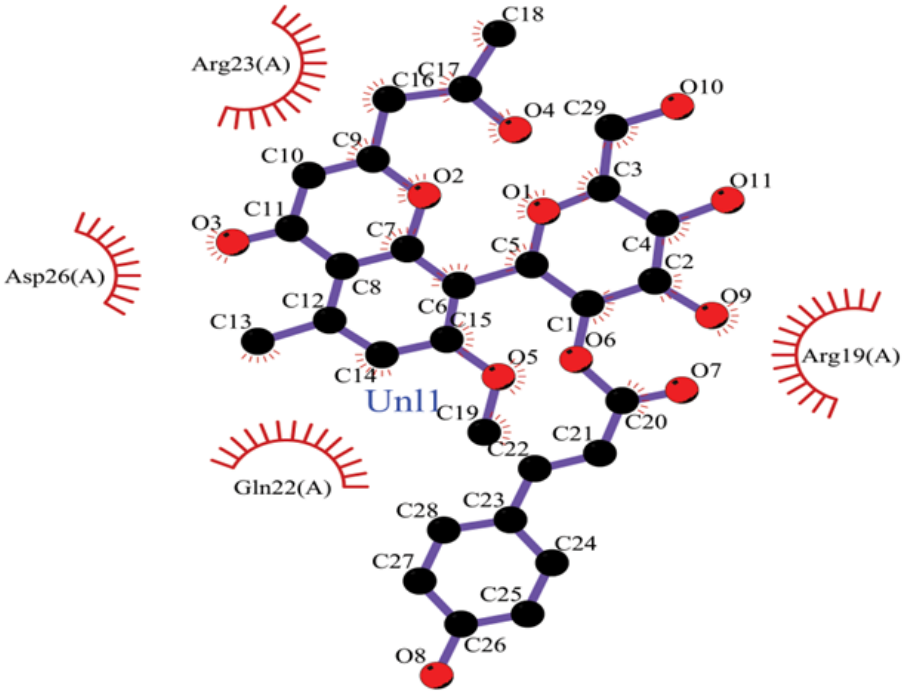

FIGURE 4.20: Interaction of Isoaloeresin D with the receptor protein

IsoaloeresinD shows hydrophobic interactions with Phe27,Asp26,Arg19,Gln22,Ile24 and forms bond with Arg23 at distance of 3.08.

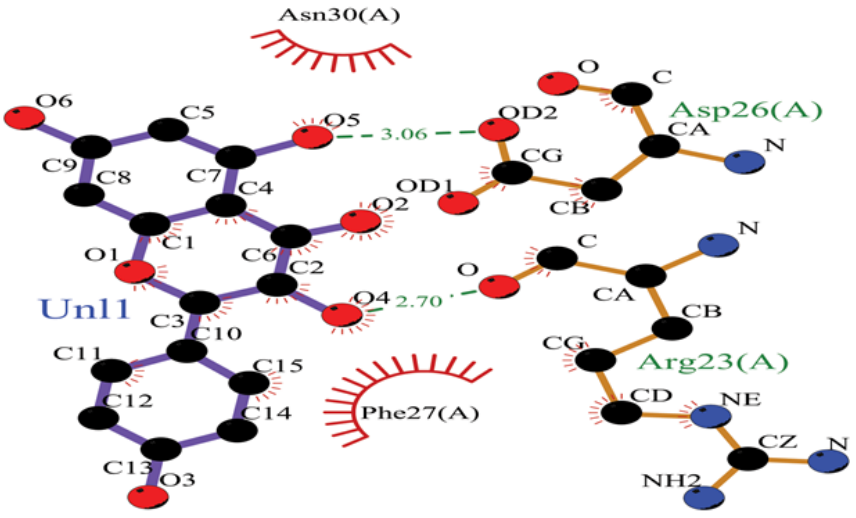

FIGURE 4.21: Interaction of Kaempferol with the receptor protein

Kaempferol shows hydrophobic interactions with Ile24, Phe27,Asn30,Arg23 and it forms bond with Asp26 at 3.77

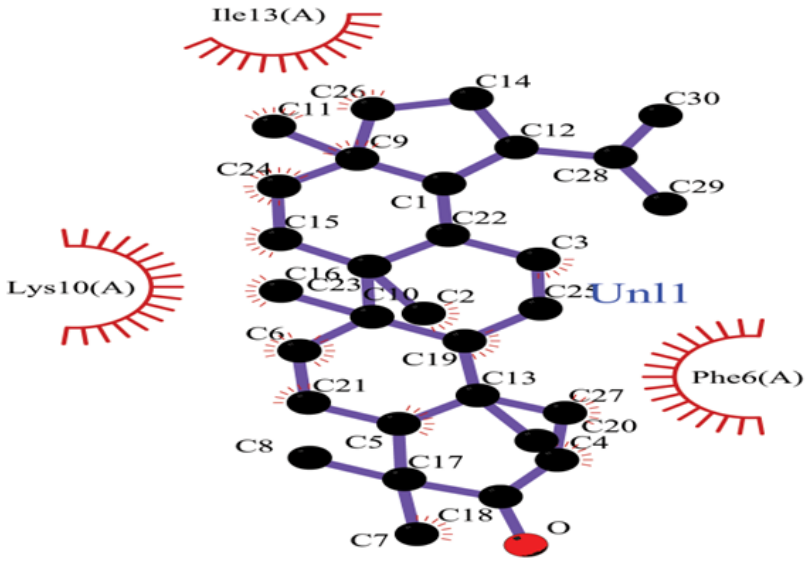

FIGURE 4.22: Interaction of Lupeol with the receptor protein

Lupeol forms no conventional hydrogen bonds, but exhibits hydrophobic interactions with Ile13(A), Lys10(A), and Phe6(A), indicating moderate binding affinity within the active pocket of the receptor.

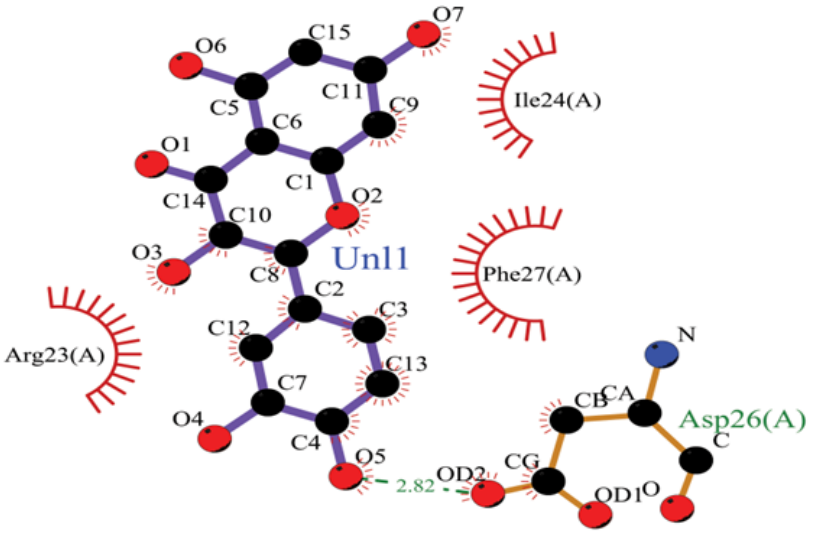

FIGURE 4.23: Interaction of Quercetin with the receptor protein

Quercetin forms a hydrogen bond with Asp26(A) at a distance of 2.82 Å. Additionally, it displays hydrophobic interactions with Arg23(A), Ile24(A), and Phe27(A), supporting a stable and specific binding conformation within the active site.

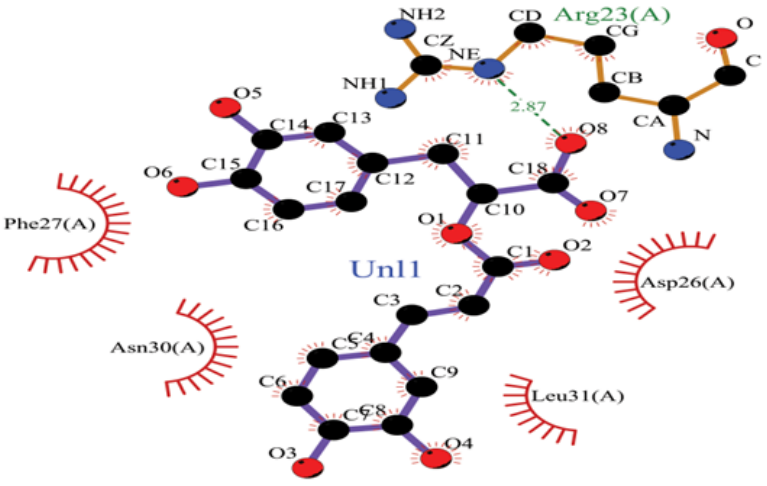

FIGURE 4.24: Interaction of Rosmarinic Acid with the receptor protein

Rosmarinic acid shows hydrophobic interactions with Asp26, Phe27,Ile24,Arg23 and it forms bond with Asn30 at Distance of 2.89.

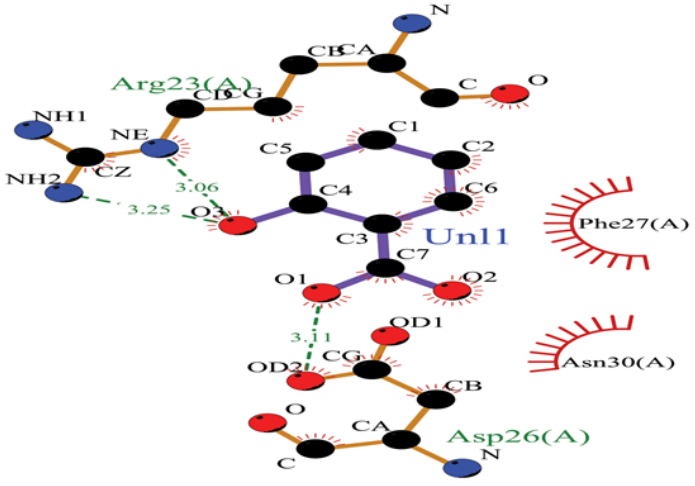

FIGURE 4.25: Interaction of Salicylic Acid with the receptor protein

Salicylic Acid shows hydrophobic interactions with Asn30, Phe27 and froms bond with Asp26 at 3.11 and forms two bond with Arg23 at distance of 3.05 and 3.25

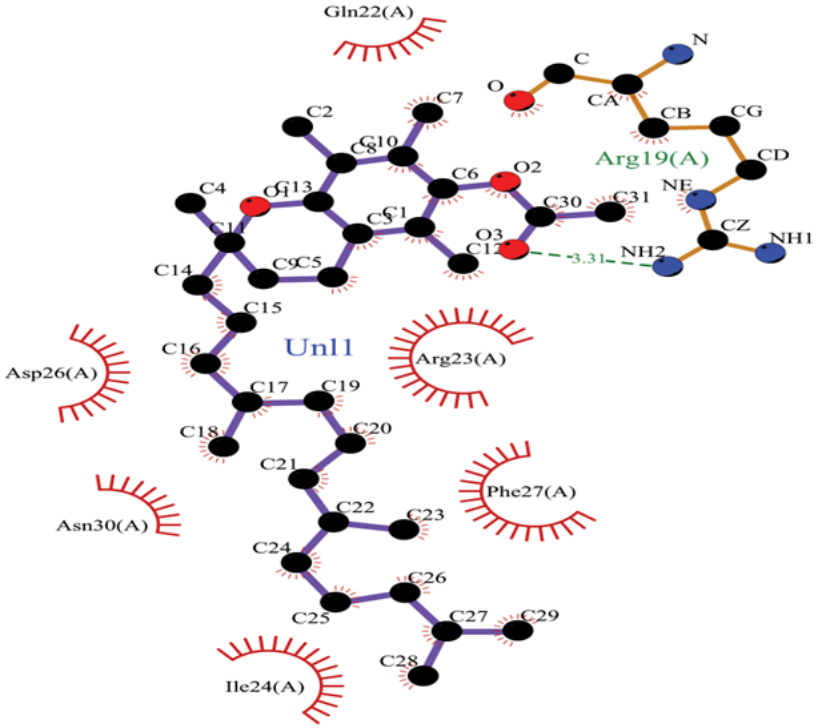

FIGURE 4.26: Interaction of Vitamin E Acetate with the receptor protein

Vitamin Eacetate shows hydrophobic interactions with Phe27, Ile24, Arg23, Arg19, Gln22, Asp26.

4.6 ADME Properties of Ligand

Lipinski's five drug law is used as a first step for the assessment of availability either verbal or artificial. pkCSM is the second tool that is used for the assessment of ADME properties [83, 84].

4.6.1 Pharmacodynamics

One of the broader terms used in pharmacology is pharmacodynamics which deals with the study of drug effects on the body.

4.6.2 Pharmacokinetics

The other term used in pharmacology is pharmacokinetics which deals with the study of the effect of the body on the drug, that how the body reacts after the drug enters the body. The absorption, distribution, metabolism, and excretion of drugs are also studies.

4.6.3 Absorption

The $CaCO_2$ solubility helps in predicting the absorption of the drugs which are administered orally. Value >0.90 (log Papp in 10^{-6} cm/s) is considered as high $CaCO_2$ permeability [85]. The water solubility of the ligands is given as log mol/L. this indicates the compound solubility in water at 25^{o}C. hence the lipid-soluble drugs will be less soluble than the water-soluble drugs [86]. Intestinal absorption indicates the value or proportion of the compound that will absorb into the intestines. A value less than 30% is considered poorly absorbed-glycoprotein is an ABC transporter that functions to extrude toxins or other xenobiotics from the cells by acting as a biological barrier [85]. P-glycoprotein inhibition can be a therapeutic target or it can act in contradiction [87]. Skin permeability is important for developing transdermal drugs. Any compound with a value > -2.5 has a low skin permeability [88]. The detailed absorption properties of five representative ligands are presented in Table 4.13, highlighting their suitability or limitations for oral or transdermal drug development.

TABLE 4.13: Absorption properties of Hexadecanoic Acid, Aloin A, Aloe emodin, Chrysophanic Acid, Glucomannan

Property	**Hexadecanoic acid**	**Aloin A**	**Aloe emodin**	**Chrysophanic acid**	**Glucomannan**
Aqueous Solubility (log mol/L)	-5.702	-3.184	-2.653	-3.077	-2.337
Caco-2 Cell Permeability (log Papp)	1.476	-0.311	-2.653	1.298	-2.337

continued on next page

Table 4.13 continued from previous page

Property	**Hexadecanoic acid**	**Aloin A**	**Aloe emodin**	**Chrysophanic acid**	**Glucomannan**
Human Intestinal Uptake (%)	91.551	49.874	80.162	96.558	15.719
Dermal Penetration (log Kp)	-2.593	-2.993	-3.731	-2.83	-2.735
P-gp Substrate Status	+	+	+	+	+
P-gp Inhibitor Type I	-	-	-	-	-
P-gp Inhibitor Type II	-	-	-	-	-

In this table "+" indicates Yes and "-" indicates No.

In Table 4.14, the absorption-related properties of five ligands—D-mannopyranose 6-phosphate, Aloesin, Isoaloeresin D, Aloeresin A, and Campesterol—are presented. The data reveal that Campesterol has the highest Caco-2 cell permeability (1.205) and intestinal uptake (94.757%), indicating its superior absorption profile. In contrast, D-mannopyranose 6-phosphate exhibits the lowest water solubility and permeability. Interestingly, Aloesin, Isoaloeresin D, and Aloeresin A act as P-gp substrates and inhibitors, suggesting potential drug-drug interaction effects.

TABLE 4.14: Absorption properties of D-mannopyranose 6-phosphate, Aloesin, Isoaloeresin D, Aloeresin A, Campesterol

Property	**D - mannopyranose 6 - phosphate**	**Aloesin**	**Isoaloeresin D**	**Aloeresin A**	**Campesterol**
Aqueous Solubility (log mol/L)	-0.811	-2.309	-3.387	-3.165	-6.818
Caco-2 Cell Permeability (log Papp)	-0.341	0.305	0.16	0.111	1.205
Human Intestinal Uptake	35.51	46.247	56.219	51.438	94.757

Table 4.14 continued from previous page

Property	**D-mannopyranose 6-phosphate**	**Aloesin**	**Isoaloeresin D**	**Aloeresin A**	**Campesterol**
Dermal Penetration (log Kp)	-2.82	-2.736	-2.736	-2.735	-2.81
P-gp Substrate Status	-	+	+	+	-
P-gp Inhibitor Type I	-	-	+	+	-
P-gp Inhibitor Type II	-	-	-	-	+

In this table "+" indicates Yes and "-" indicates No.

TABLE 4.15: Absorption properties of Lupeol, Salicylic Acid, Caffeic Acid, Ferulic Acid, Gallic Acid

Property	**Lupeol**	**Salicylic Acid**	**Caffeic Acid**	**Ferulic Acid**	**Gallic Acid**
Aqueous Solubility (log mol/L)	-5.861	-1.808	-2.33	-2.817	-2.56
Caco-2 Cell Permeability (log Papp)	1.226	1.151	0.634	0.176	-0.081
Human Intestinal Uptake (%)	95.782	83.887	69.407	93.685	43.374
Dermal Penetration (log Kp)	-2.744	-2.723	-2.722	-2.72	-2.735
P-gp Substrate Status	-	-	-	-	-
P-gp Inhibitor Type I	+	-	-	-	-
P-gp Inhibitor Type II	+	-	-	-	-

In this table "+" indicates Yes and "-" indicates No.

Table 4.15 highlights the absorption properties of Lupeol, Salicylic Acid, Caffeic acid, Ferulic acid, and Gallic Acid. Lupeol stands out with excellent intestinal uptake (95.782%) and high Caco-2 permeability (1.226). On the other hand, Gallic acid shows relatively poor permeability and uptake. Notably, Lupeol also acts as both P-gp inhibitor Type I and II, which could affect the bioavailability of co-administered drugs. In this table "+" indicates Yes and "-" indicates No.

TABLE 4.16: Absorption properties of Kaempferol, Quercetin, Apigenin, Cycloartenol, Ascorbic Acid

Property	**Kaempferol**	**Quercetin**	**Apigenin**	**Cycloartenol**	**Ascorbic Acid**
Aqueous Solubility (log mol/L)	-3.04	-2.925	-3.329	-5.762	-1.556
Caco-2 Cell Permeability (log Papp)	0.032	-0.229	1.007	1.194	-0.255
Human Intestinal Uptake (%)	74.29	77.207	93.25	95.248	39.154
Dermal Penetration (log Kp)	-2.735	-2.735	-2.735	-2.737	-2.955
P-gp Substrate Status	+	+	+	-	-
P-gp Inhibitor Type I	-	-	-	+	-
P-gp Inhibitor Type II	-	-	-	+	-

In this table "+" indicates Yes and "-" indicates No.

TABLE 4.17: Absorption properties of Vitamin E Acetate, Folic Acid, Aloesaponarin I, Aloesaponarin II, Rosmarinic Acid

Property	**Vitamin E Acetate**	**Folic Acid**	**Aloesaponarin I**	**Aloesaponarin II**	**Rosmarinic Acid**
Aqueous Solubility (log mol/L)	-8.176	-2.88	-3.312	-3.095	-3.059
Caco-2 Cell Permeability (log Papp)	1.198	-0.877	0.293	1.047	-0.937
Human Intestinal Uptake (%)	92.117	1.108	84.791	94.683	32.516
Dermal Penetration (log Kp)	-2.774	-2.735	-2.789	-3.437	-2.735
P-gp Substrate Status	-	+	+	+	+
P-gp Inhibitor Type I	+	-	-	-	-
P-gp Inhibitor Type II	+	-	-	-	-

In this table "+" indicates Yes and "-" indicates No.

4.6.3.1 Distribution

TABLE 4.18: Distribution properties of Hexadecanoic Acid, Aloin A, Aloe emodin, Chrysophanic Acid, Glucomannan

Property	**Hexadecanoic acid**	**Aloin A**	**Aloe emodin**	**Chryso-phanic acid**	**Glucoman-nan**
Volume of Distribution in Humans (VDss, log L/kg)	0.159	-0.991	-0.706	0.272	-0.53
Unbound Drug Fraction in Plasma (Human)	0.186	0.405	0.286	0.154	0.415
Blood–Brain Barrier Permeability (log BB)	0.028	-1.065	-0.667	0.212	-1.753
Central Nervous System Penetration (log PS)	-1.307	-3.91	-2.422	-2.111	-6.166

TABLE 4.19: Distribution properties of D-mannopyranose 6-phosphate, Aloesin, Isoaloeresin D, Aloeresin A, Campesterol

Property	**D-manno-pyranose 6 - phosphate**	**Aloesin**	**Isoaloeresin D**	**Aloeresin A**	**Campesterol**
Volume of Distribution in Humans	0.144	0.212	0.076	0.392	0.29
Unbound Drug Fraction in Plasma (Human)	0.716	0.416	0.04	0.058	0
Blood–Brain Barrier Permeability (log BB)	-1.414	-1.29	-1.585	-1.669	0.771
Central Nervous System Penetration (log PS)	-4.211	-3.783	-3.584	-3.555	-1.805

TABLE 4.20: Distribution Properties of Lupeol, Salicylic Acid, Caffeic Acid, Ferulic Acid, Gallic Acid

Property	**Lupeol**	**Salicylic Acid**	**Caffeic acid**	**Ferulic acid**	**Gallic Acid**
Volume of Distribution in Humans	0	-1.57	-1.098	-1.367	-1.855
Unbound Drug Fraction in Plasma (Human)	0	0.563	0.529	0.343	0.617

Table 4.20 continued from previous page

Property	**Lupeol**	**Salicylic Acid**	**Caffeic acid**	**Ferulic acid**	**Gallic Acid**
Blood–Brain Barrier Permeability (log BB)	0.726	-0.334	-0.647	-0.239	-1.102
Central Nervous System Penetration (log PS)	-1.714	-3.21	-2.608	-2.612	-3.74

TABLE 4.21: Distribution properties of Kaempferol, Quercetin, Apigenin, Cycloartenol, Ascorbic Acid

Property	**Kaempferol**	**Quercetin**	**Apigenin**	**Cycloartenol**	**Ascorbic Acid**
Volume of Distribution in Humans (VDss, log L/kg)	1.274	1.559	0.822	-0.075	0.218
Unbound Drug Fraction in Plasma (Human)	0.178	0.206	0.147	0	0.825
Blood – Brain Barrier Permeability (log BB)	-0.939	-1.098	-0.734	0.794	-0.985
Central Nervous System Penetration (log PS)	-2.228	-3.065	-2.061	-1.714	-3.217

TABLE 4.22: Distribution properties of Vitamin E Acetate, Folic Acid, Aloesaponarin I, Aloesaponarin II, Rosmarinic Acid

Property	**Vitamin E acetate**	**Folic Acid**	**Aloesaponarin I**	**Aloesaponarin II**	**Rosmarinic acid**
Volume of Distribution in Humans	0.79	0.046	-0.081	-0.568	0.393
Unbound Drug Fraction in Plasma	0	0.37	0.165	0.227	0.348
Blood–Brain Barrier Permeability	-0.275	-1.615	-0.099	-0.01	-1.378
Central Nervous System Penetration	-1.724	-4.262	-3.14	-2.024	-3.347

4.6.3.2 Metabolism

TABLE 4.23: Metabolic properties of Hexadecanoic Acid, Aloin A, Aloe emodin, Chrysophanic Acid, Glucomannan

Ligands	**Hexadecanoic acid**	**Aloin A**	**Aloe emodin**	**Chrysophanic acid**	**Glucomannan**
CYP2D6 Substrate	-	-	-	-	-
CYP3A4 Substrate	-	+	-	-	-
Inhibits CYP1A2	+	-	+	+	-
Inhibits CYP2C19	-	-	-	-	-
Inhibits CYP2C9	-	-	-	-	-
Inhibits CYP2D6	-	-	-	-	-
Inhibits CYP3A4	-	-	-	-	-

In this table "+" indicates Yes and "-" indicates No.

TABLE 4.24: Metabolic properties of D-mannopyranose 6-phosphate, Aloesin, Isoaloeresin D, Aloeresin A, Campesterol

Ligands	**D-manno pyranose 6-phosphate**	**Aloesin**	**Isoaloeresin D**	**Aloeresin A**	**Campesterol**
CYP2D6 Substrate	-	-	-	-	-
CYP3A4 Substrate	-	-	+	+	+
Inhibits CYP1A2	-	-	-	-	-
Inhibits CYP2C19	-	-	-	-	-
Inhibits CYP2C9	-	-	-	-	-
Inhibits CYP2D6	-	-	-	-	-
Inhibits CYP3A4	-	-	+	+	-

In this table "+" indicates Yes and "-" indicates No.

TABLE 4.25: Metabolic properties of Lupeol, Salicylic Acid, Caffeic Acid, Ferulic Acid, Gallic Acid

Ligands	**Lupeol**	**Salicylic Acid**	**Caffeic acid**	**Ferulic acid**	**Gallic Acid**
Acts as CYP2D6 Substrate	-	-	-	-	-
Acts as CYP3A4 Substrate	+	-	-	-	-
Inhibits CYP1A2	-	-	-	-	-

Table 4.25 continued from previous page

Ligands	**Lupeol**	**Salicylic Acid**	**Caffeic acid**	**Ferulic acid**	**Gallic Acid**
Inhibits CYP2C19	-	-	-	-	-
Inhibits CYP2C9	-	-	-	-	-
Inhibits CYP2D6	-	-	-	-	-
Inhibits CYP3A4	-	-	-	-	-

In this table "+" indicates Yes and "-" indicates No.

TABLE 4.26: Metabolic properties of Kaempferol, Quercetin, Apigenin, Cycloartenol, Ascorbic Acid

Ligands	**Kaempferol**	**Quercetin**	**Apigenin**	**Cycloartenol**	**Ascorbic Acid**
Acts as CYP2D6 Substrate	-	-	-	-	-
Acts as CYP3A4 Substrate	-	-	-	+	-
Inhibits CYP1A2	+	+	+	-	-
Inhibits CYP2C19	-	-	+	-	-
Inhibits CYP2C9	-	-	-	-	-
Inhibits CYP2D6	-	-	-	-	-
Inhibits CYP3A4	-	-	-	-	-

In this table "+" indicates Yes and "-" indicates No.

TABLE 4.27: Metabolic properties of Vitamin E Acetate, Folic Acid, Aloesaponarin I, Aloesaponarin II, Rosmarinic Acid

Ligands	**Vitamin E acetate**	**Folic Acid**	**Aloesaponarin I**	**Aloesaponarin II**	**Rosmarinic acid**
Acts as CYP2D6 Substrate	-	-	-	-	-
Acts as CYP3A4 Substrate	+	-	-	-	-
Inhibits CYP1A2	-	-	-	+	-
Inhibits CYP2C19	-	-	-	-	-

In this table "+" indicates Yes and "-" indicates No.

Table 4.27 continued from previous page

Ligands	**Vitamin E ac-etate**	**Folic Acid**	**Aloesaponarin I**	**Aloesaponarin II**	**Rosmarinic acid**
Inhibits CYP2C9	-	-	-	-	-
Inhibits CYP2D6	-	-	-	-	-
Inhibits CYP3A4	-	-	-	-	-

In this table "+" indicates Yes and "-" indicates No.

4.6.3.3 Excretion

TABLE 4.28: Excretory properties of Hexadecanoic Acid, Aloin A, Aloe emodin, Chrysophanic Acid, Glucomannan

Ligands	**Hexadecanoic acid**	**Aloin A**	**Aloe emodin**	**Chrysophanic acid**	**Glucomannan**
Predicted Total Drug Clearance	1.565	0.921	-0.006	0.020	1.878
Renal Organic Cation Transporter 2 (OCT2) Substrate Status	-	-	-	-	-

In this table "+" indicates Yes and "-" indicates No.

TABLE 4.29: Excretory properties of D-mannopyranose 6-phosphate, Aloesin, Isoaloeresin D, Aloeresin A, Campesterol

Ligands	**D-manno pyranose 6-phosphate**	**Aloesin**	**Isoaloeresin D**	**Aloeresin A**	**Campesterol**
Predicted Total Drug Clearance	0.414	0.456	0.500	0.366	0.572
Renal Organic Cation Transporter 2 (OCT2) Substrate Status	-	-	-	-	-

In this table "+" indicates Yes and "-" indicates No.

TABLE 4.30: Excretory properties of Lupeol, Salicylic Acid, Caffeic Acid, Ferulic Acid, Gallic Acid

Ligands	**Lupeol**	**Salicylic Acid**	**Caffeic acid**	**Ferulic acid**	**Gallic Acid**
Predicted Total Drug Clearance	0.153	0.607	0.508	0.623	0.518
Renal Organic Cation Transporter 2 (OCT2) Substrate Status	-	-	-	-	-

In this table "+" indicates Yes and "-" indicates No.

TABLE 4.31: Excretory properties of Kaempferol, Quercetin, Apigenin, Cycloartenol, Ascorbic Acid

Ligands	**Kaempferol**	**Quercetin**	**Apigenin**	**Cycloartenol**	**Ascorbic Acid**
Predicted Total Drug Clearance	0.477	0.407	0.566	0.262	0.631
Renal Organic Cation Transporter 2 (OCT2)	-	-	-	-	-

In this table "+" indicates Yes and "-" indicates No.

TABLE 4.32: Excretory properties of Vitamin E Acetate, Folic Acid, Aloesaponarin I, Aloesaponarin II, Rosmarinic Acid

Ligands	**Vitamin E acetate**	**Folic Acid**	**Aloesaponarin I**	**Aloesaponarin II**	**Rosmarinic acid**
Predicted Total Drug Clearance	0.808	0.527	0.164	0.049	0.25
Renal Organic Cation Transporter 2 (OCT2)	-	-	-	-	-

In this table "+" indicates Yes and "-" indicates No.

4.7 Lead Compound Identification

Based on comprehensive screening that includes physicochemical properties, pharmacokinetics, toxicity profiles, and molecular docking results, Apigenin has been

identified as the most suitable lead compound in this study. Initially, 25 ligands were selected and assessed against Lipinski's Rule of Five, which serves as the first filter in drug-likeness evaluation [89, 90]. Compounds such as Glucomannan, Isoaloeresin D, and Aloeresin A were ruled out in this stage due to multiple violations, particularly with high molecular weight and excessive hydrogen bond donors or acceptors. Apigenin, on the other hand, satisfied all criteria of Lipinski's rule with a molecular weight of 270.24 g/mol, Log P value of 2.5768, 5 hydrogen bond acceptors, and 3 hydrogen bond donors, indicating high oral bioavailability potential [91].

In the second screening step, toxicity prediction was carried out using various models including AMES test, hepatotoxicity, hERG inhibition, and more. Apigenin passed all toxicity filters showing no mutagenic, hepatotoxic, or cardiotoxic properties making it a safe candidate. Its pharmacokinetic profile was also favorable, with high human intestinal absorption (93.25%), adequate $CaCO_2$ permeability (1.007), and reasonable total clearance (0.566 mL/min/kg), indicating efficient absorption and elimination. Furthermore, it is not a P-glycoprotein inhibitor or substrate, reducing the risk of drug efflux or interactions [92].

From a pharmacodynamic and molecular docking perspective, Apigenin showed strong binding affinity with the receptor protein used in this study, with a Vina binding score of -5.1 kcal/mol and a large cavity size of 19, suggesting a stable and significant interaction. While other compounds like Isoaloeresin D and Vitamin E acetate showed slightly better docking scores (-6.6 and -6.2 respectively), they were eliminated due to poor ADME profiles or toxicity issues such as hERG II inhibition and low water solubility.

Considering all evaluation parameters—drug-likeness, toxicity, pharmacokinetics, and molecular docking Apigenin stands out as the most viable lead compound for further drug development. Kaempferol is proposed as a strong secondary candidate due to its balanced safety and efficacy profiles. Both compounds hold significant potential for advancement in therapeutic research and drug design [92, 93].

4.8 Drug Identification for Rosacea Treatment

Among the various treatment strategies for rosacea, Doxycycline an FDA-approved tetracycline antibiotic has shown significant effectiveness in reducing the inflammatory symptoms of the disease. Its therapeutic use is primarily attributed to its anti-inflammatory, rather than antibacterial, properties. Low-dose Doxycycline (commonly 40 mg/day) is widely used in the United States, Pakistan, India, and other countries for managing papulopustular rosacea, especially in adults. It has demonstrated the ability to reduce facial lesions and erythema without contributing significantly to antibiotic resistance. Despite its widespread clinical use, ongoing research and clinical evaluations continue to optimize its dosage and long-term safety profile [94].

4.8.1 Doxycycline

Doxycycline is a second-generation, broad-spectrum antibiotic belonging to the tetracycline class, widely used for the treatment of various bacterial infections, including respiratory tract infections, urinary tract infections, acne, chlamydia, Lyme disease, and as a prophylactic agent against malaria. It exerts its antibacterial effect by inhibiting bacterial protein synthesis through binding to the 30S ribosomal subunit, thereby preventing the incorporation of amino acids into the growing peptide chain. Compared to earlier tetracyclines, doxycycline offers improved oral bioavailability, an extended half-life, and superior tissue penetration [96].

Beyond its antimicrobial function, doxycycline is well known for its anti - inflammatory properties, making it beneficial in the treatment of several non-infectious inflammatory disorders such as rosacea, periodontitis, and rheumatoid arthritis. In the context of rosacea, a chronic inflammatory skin disorder, doxycycline not only targets microbial agents like Demodex mites and Bacillus oleronius but also modulates the host's innate immune response. A key player in rosacea pathophysiology is the cathelicidin peptide LL-37, which, when abnormally processed,

promotes inflammation, vasodilation, and tissue damage. Doxycycline inhibits matrix metalloproteinases (MMPs), particularly MMP-9, which are responsible for the pathological cleavage of cathelicidin into its active LL-37 form. By suppressing MMP activity, doxycycline reduces LL-37 expression and interrupts the inflammatory cascade, positioning it as a modulator of innate immunity in addition to its antibiotic role [95].

Doxycycline is also used as a reference compound in molecular docking studies to evaluate the binding efficiency of novel therapeutic agents such as catharadine, a plant-derived alkaloid, which may also interact with LL-37-related pathways. Due to its dual mechanism of action, favorable pharmacokinetic profile, and broad therapeutic applications, doxycycline remains a cornerstone drug in both clinical practice and biomedical research [95].

4.9 Drug ADMET Properties

4.9.1 Toxicity Predication of Reference Drug

The toxicity profile of Doxycycline, summarized in Table 4.33, indicates a favorable safety margin. The drug tested negative in the AMES toxicity model, suggesting no mutagenic potential. It is also non-inhibitory to hERG I and II channels, implying a low risk of cardiotoxicity. Additionally, no hepatotoxicity or skin sensitization was predicted. Acute and chronic oral toxicity in rats were found to be 2.23 and 3.073 (log mg/kg/day), respectively. Toxicity toward Tetrahymena pyriformis and minnows was 0.285 log μg/L and 4.509 log mM, respectively, showing low environmental toxicity.

TABLE 4.33: Toxicity predication of reference drug

S.No	Model Name	Predicted Value
1	AMES Mutagenicity Test	-
2	Maximum Tolerated Dose in Humans (log mg/kg/day)	0.294
3	hERG Channel Blocker – Type I	-
4	hERG Channel Blocker – Type II	-

Table 4.33 continued from previous page

S.No	Model Name	Predicted Value
5	Acute Oral Toxicity in Rats (LD_{50}, log mol/kg)	2.23
6	Chronic Oral Toxicity in Rats (LOAEL, log mg/kg bw/day)	3.073
7	Liver Toxicity Potential (Hepatotoxicity)	-
8	Potential for Skin Allergy (Sensitization)	-
9	*T. pyriformis Toxicity (log µg/L)*	0.285
10	Minnow Toxicity – LC_{50} (log mM)	4.509

In this table Toxicity predication of reference drug "+" indicates Yes and "-" indicates No.

4.9.2 Absorption Properties of Reference Drug

The absorption characteristics of Doxycycline, given in Table 4.34, show moderate intestinal absorption (44.517%), though the low $CaCO_2$ permeability (0.154) suggests limited passive transcellular transport. The negative water solubility value (-2.449 log mol/L) indicates moderate aqueous solubility. Doxycycline is a substrate for P-glycoprotein, indicating it may be subject to efflux transport, but it does not inhibit P-gp I or II.

TABLE 4.34: Absorption properties of reference drug

S. No.	Reference drug	Doxycycline
1	Aqueous Solubility (log mol/L)	-2.449
2	Caco-2 Cell Permeability (log Papp)	0.154
3	Human Intestinal Uptake (%)	44.517
4	Dermal Penetration (log Kp)	-2.735
5	P-gp Substrate Status	+
6	P-gp Inhibitor Type I	-
7	P-gp Inhibitor Type II	-

In this table it shows Absorption properties of reference drug "+" indicates Yes and "-" indicates No.

4.9.3 Distribution Properties of Reference Drug

As illustrated in Table 4.35, the volume of distribution at steady state (VDss) of Doxycycline is 1.137 log L/kg, indicating moderate tissue penetration. The

fraction unbound (0.499) suggests about half of the drug remains free in systemic circulation. The low BBB (-0.802) and CNS permeability (-3.958) values imply that Doxycycline poorly penetrates the central nervous system, making it unsuitable for CNS-targeted treatments.

TABLE 4.35: Distribution properties of reference drug

S. No.	Reference Drug	Doxycycline
1	Volume of Distribution in Humans (VDss, log L/kg)	1.137
2	Unbound Drug Fraction in Plasma (Human)	0.499
3	Blood–Brain Barrier Permeability (log BB)	-0.802
4	Central Nervous System Penetration (log PS)	-3.958

4.9.4 Metabolism

As shown in Table 4.36, Doxycycline does not act as a substrate or inhibitor for major cytochrome P450 isoenzymes including CYP2D6, CYP3A4, CYP1A2, CYP2C19, and CYP2C9. This suggests a lower likelihood of drug–drug interactions via hepatic enzyme inhibition or metabolism.

4.9.4.1 Metabolic Properties of Reference Drug

TABLE 4.36: Metabolic properties of reference drug

S. No	Reference Drug	Doxycycline
1	Acts as CYP2D6 Substrate	-
2	Acts as CYP3A4 Substrate	-
3	Inhibits CYP1A2	-
4	Inhibits CYP2C19	-
5	Inhibits CYP2C9	-
6	Inhibits CYP2D6	-
7	Inhibits CYP3A4	-

Table show Metabolic properties of reference drug “+” indicates Yes & “-” indicates No.

4.9.5 Excretion

The excretion profile presented in Table 4.37 indicates a total clearance value of 0.215 mL/min/kg, suggesting a moderate rate of elimination. Moreover, Doxycycline is not a substrate of renal OCT2, which implies reduced likelihood of renal transporter-mediated excretion.

TABLE 4.37: Excretory properties of reference drug

S. No.	Reference Drug	Doxycycline
1	Predicted Total Drug Clearance (log mL/min/kg)	0.215
2	Renal Organic Cation Transporter 2 (OCT2) Substrate Status	-

In this table Excretory properties of reference drug "+" indicates Yes and "-" indicates No.

4.10 Doxycycline Mechanism of Action

Doxycycline is a broad-spectrum antibiotic from the tetracycline class that works by inhibiting bacterial protein synthesis, thereby exerting a bacteriostatic effect. Doxycycline penetrates bacterial cells via both passive diffusion and active transport. Inside the cell, it reversibly attaches to the 30S ribosomal subunit. This binding inhibits the attachment of aminoacyl-tRNA to the A site of the mRNA-ribosome complex, thereby blocking the addition of new amino acids to the elongating peptide chain. Consequently, protein synthesis is interrupted, leading to the inhibition of bacterial growth [97].

4.11 Effects of Doxycycline on the Human Body

Doxycycline exerts both beneficial as well as adverse effects on the human body. As a broad-spectrum antibiotic, its primary therapeutic role is to treat various bacterial infections, including respiratory tract infections, urinary tract infections, sexually transmitted infections, acne, and vector-borne diseases like Lyme disease and malaria. It also has notable anti-inflammatory properties, making it effective in treating inflammatory skin conditions such as acne and rosacea. Doxycycline is

well absorbed and penetrates tissues effectively, including the lungs, prostate, and intracellular sites, enhancing its usefulness in difficult-to-reach infections. Additionally, it is used in certain parasitic diseases due to its action on intracellular symbionts like Wolbachia [97].

Despite its therapeutic value, doxycycline can cause side effects. Gastrointestinal disturbances such as nausea, vomiting, diarrhea, and esophageal irritation are common, especially if the drug is taken without sufficient water or while lying down. A well-known side effect is photosensitivity, where the skin becomes more sensitive to sunlight, increasing the risk of sunburn. In children under 8 years and during pregnancy, doxycycline can cause permanent discoloration of developing teeth and affect bone growth, which is why it is contraindicated in these groups. Although rare, liver toxicity and hypersensitivity reactions such as rash or allergic responses may occur. It may also disrupt normal body flora, leading to overgrowth of fungi and resulting in oral or vaginal thrush. Unlike other tetracyclines, doxycycline is safer in patients with kidney disease because it does not accumulate in the kidneys. To ensure optimal absorption and minimize side effects, patients are advised to avoid taking it with dairy products, antacids, or iron supplements, which can interfere with its absorption [97]. The molecular docking analysis of Doxycycline with the LL-37 antimicrobial peptide revealed a binding score of -5.8, indicating a moderate binding affinity. The cavity size was measured at 19 $Å^3$, and the molecule possessed 6 hydrogen bond donors (HBD) and 9 hydrogen bond acceptors (HBA). With a logP of -0.5042, Doxycycline shows hydrophilic characteristics, and its molecular weight was calculated as 444.44 g/mol (see Table 4.38).

TABLE 4.38: Docking of Doxycycline with LL37.

Compound	**Binding Score**	**Cavity size**	**HBD**	**HBA**	**logP**	**Molecular Weight g/mol**
Doxycycline	-5.8	19	6	9	-0.5042	444.44

4.12 Doxycycline Comparison with Lead Compound

The standard drug azithromycin is compared with the lead compound apigenin by evaluating their physicochemical and pharmacokinetic properties to assess bioavailability, efficacy, safety, and drug-likeness.

As illustrated in Figure 4.28, Apigenin exhibits a higher log P-value (2.5768) compared to Doxycycline (-0.5042), indicating greater lipophilicity, which may enhance membrane permeability. However, Doxycycline has a higher molecular weight (444.44 g/mol) than Apigenin (270.24 g/mol), which could influence absorption and distribution. Doxycycline also shows a higher number of hydrogen bond acceptors (9) and donors (6) compared to Apigenin (5 acceptors and 3 donors), suggesting it may form more stable interactions with biological targets, though potentially at the cost of reduced membrane permeability.

Table 4.39: Doxycycline comparison with lead compound.

Name of Compound	**Log P-value**	**Molecular Weight g/mol**	**H-bond acceptor**	**H-bond donor**
Doxycycline	-0.5042	444.44	9	6
Apigenin	2.5768	270.24	5	3

4.13 ADMET Properties Comparison

The comparison of ADMET properties is conducted to evaluate the absorption, distribution, metabolism, excretion, and toxicity of both the drug and the lead compound, aiming to identify a superior drug candidate.

4.13.1 Toxicity Comparison

The toxicity of both the standard drug and the lead compound is evaluated using nine different models. Model 1, the AMES toxicity test, indicates that neither

the standard drug nor the lead compound is mutagenic. Model 2 assesses the Maximum Tolerated Dose (MTD), where a value of 0.477 log mg/kg/day or less is considered low, and higher values are considered high. According to the table, apigenin has a low tolerated dose value. The third model evaluates hERG I and II inhibition, revealing that neither compound acts as an inhibitor. Model 4 measures oral acute toxicity in rats to assess relative toxicity, while Model 5 examines oral chronic toxicity by determining the lowest dose that may cause adverse effects. Model 6 assesses hepatotoxicity, indicating potential liver damage; the data show that azithromycin is hepatotoxic. Model 7 tests dermal sensitivity, showing that both compounds are not sensitive to skin. Model 8 uses *T. pyriformis* to evaluate toxicity, where a value greater than -0.5 is considered toxic; azithromycin shows some toxicity in this test. Finally, Model 9 assesses minnow toxicity, with values below 0.5 mM considered toxic; both compounds pass this test.

Table 4.40: Toxicity Comparison.

Sr.	**Model Name**	**Doxycycline**	**Apigenin**
1	AMES Mutagenicity Test	-	-
2	Maximum Tolerated Dose in Humans (log mg/kg/day)	0.294	0.328
3	hERG Channel Blocker – Type I	-	-
4	hERG Channel Blocker – Type II	-	-
5	Acute Oral Toxicity in Rats (LD_{50}, log mol/kg)	2.23	2.45
6	Chronic Oral Toxicity in Rats	3.073	2.298
7	Liver Toxicity Potential (Hepatotoxicity)	-	-
8	Potential for Skin Allergy (Sensitization)	-	-
9	*T. pyriformis* Toxicity (log μg/L)	0.285	0.38
10	Minnow Toxicity – LC_{50} (log mM)	4.509	2.432

4.13.2 Absorption Properties Comparison

The absorption parameter is evaluated using six models. The water solubility model measures the compound's solubility in water at 25^oC. The $CaCO_2$ permeability model predicts oral drug absorption, where values above 0.90 indicate high intestinal absorption; chrysoplenetin shows higher absorption than azithromycin. In the intestinal absorption model, values below 30% denote poor absorption,

but both compounds demonstrate high intestinal absorption, with chrysoplenetin performing better. For transdermal drugs, the skin permeability model considers a value of log Kp greater than -2.5 as low permeability; both compounds pass this test. The P-glycoprotein substrate model is crucial since P-glycoprotein functions as an ABC transporter and biological barrier; both chrysoplenetin and azithromycin act as substrates. The final model assesses whether the compounds act as P-glycoprotein inhibitors.

Table 4.41: Absorption Properties Comparison.

Sr.	**Reference drug**	**Doxycycline**	**Apigenin**
1	Aqueous Solubility (log mol/L)	-2.449	-3.329
2	Caco-2 Cell Permeability (log Papp)	0.154	1.007
3	Human Intestinal Uptake (%)	44.517	93.25
4	Dermal Penetration (log Kp)	-2.735	-2.735
5	P-gp Substrate Status	+	+
6	P-gp Inhibitor Type I	_	_
7	P-gp Inhibitor Type II	_	_

Comparison of Absorption Properties between Reference Drug (Doxycycline) and Lead Compound (Apigenin). "+" indicates Yes and "-" indicates No.

4.13.3 Metabolic Properties Comparison

Table 4.42: Metabolic Properties Comparison

Sr.	**Reference Drug**	**Doxycycline**	**Apigenin**
1	Acts as CYP2D6 Substrate	–	–
2	Acts as CYP3A4 Substrate	–	–
3	Inhibits CYP1A2	–	+
4	Inhibits CYP2C19	–	+
5	Inhibits CYP2C9	–	–
6	Inhibits CYP2D6	–	–
7	Inhibits CYP3A4	–	–

In this table Metabolic Properties Comparison "+" indicates Yes and "_" indicates No

4.13.4 Distribution Properties Comparison

Table 4.43: Distribution Properties Comparison.

Sr.	Reference Drug	Doxycycline	Apigenin
1	Volume of Distribution in Humans (VDss, log L/kg)	1.137	0.822
2	Unbound Drug Fraction in Plasma (Human)	0.499	0.147
3	Blood–Brain Barrier Permeability (log BB)	-0.802	-0.734
4	Central Nervous System Penetration (log PS)	-3.958	-2.061

4.13.5 Excretion Properties Comparison

Table 4.44: Excretion Properties Comparison.

Sr.	Reference Drug	Doxycycline	Apigenin
1	Predicted Total Drug Clearance	0.215	0.566
2	Renal Organic Cation Transporter 2 (OCT2) Substrate Status	_	_

In this table of Excretion Properties Comparison "+" indicates Yes and "_" indicates No.

4.14 Physiochemical Properties Comparison

Table 4.45: Physiochemical Properties Comparison.

Drug	Molecular Formula	H-bond donor	H-bond acceptor	Log P-value	Molecular Weight
Doxycycline	$C_{22}H_{24}N_2O_8$	6	9	-0.5042	444.44
Apigenin	$C_{15}H_{10}O_5$	3	5	2.5768	270.24

4.15 Docking Score Comparison

Table 4.46: Docking score comparison

S.No.	Compound	Binding Score
1	Doxycycline	-5.8
2	Apigenin	-5.1

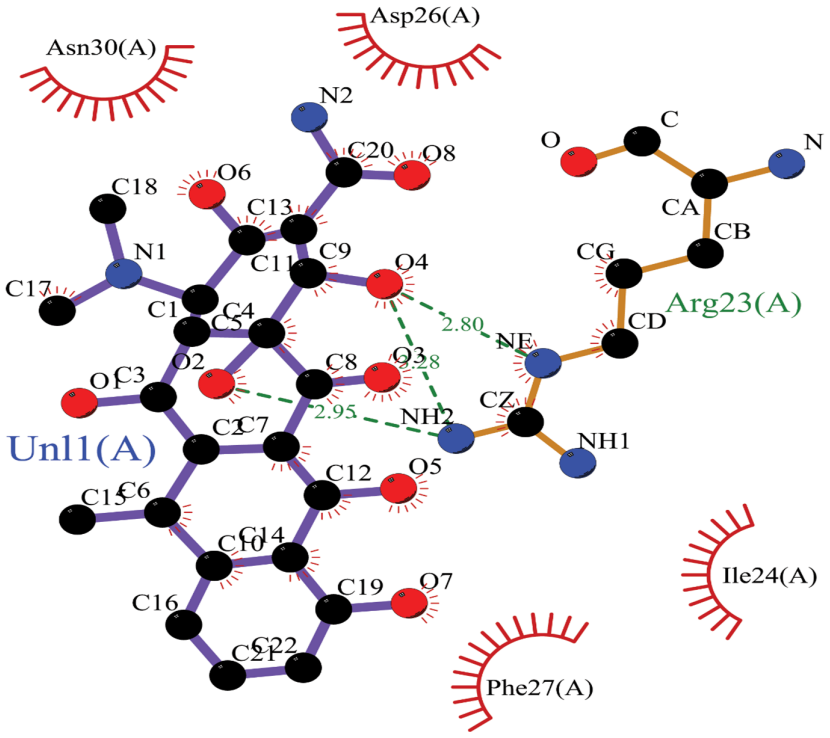

FIGURE 4.27: Docoxyciline with receptor protein

It has hydrophobic interaction between Phe27, Ile24, Asn30 and forms bond with Arg23 with a distance of 3.04, 3.05, 3.06 and Asp26 at a Distance of 3.08.

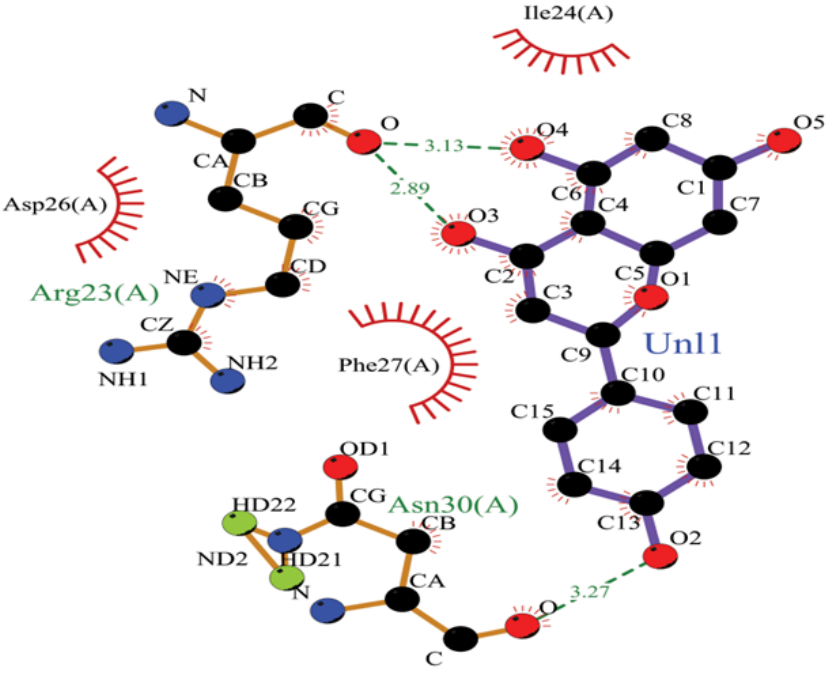

FIGURE 4.28: Apigenin with receptor protein

It forms Hydrophobic interaction with Asp26, Asn30, Ile24 and forms bond with Arg23 with a distance of 3.14 and 2.89 and forms a bond with Asn30 with 3.27.

This study was conducted to identify a potential natural therapeutic compound for the treatment of Rosacea, a chronic inflammatory skin disorder. For this purpose, LL-37, a key antimicrobial peptide implicated in the pathogenesis of Rosacea, was selected as the target protein due to its role in promoting skin inflammation via the NLRP3 inflammasome [8, 35]. The physical and chemical properties of the target protein were determined and are presented. A total of 25 bioactive constituents from Aloe vera were selected and screened for their drug-likeness [29], toxicity [25], and the results are summarized across ADME properties and binding affinity against LL-37 [49]. The 3D structures of these ligands were obtained from PubChem [48] and processed through tools like ChemDraw and Chem3D Ultra for optimization. Molecular docking was performed using CB-Dock with LL-37 [49], and interactions were visualized and analyzed through PyMOL and LigPlot [45][50]. Initial screening based on Lipinski's Rule of Five led to the elimination of several compounds such as Glucomannan and Aloeresin A due to violations in molecular weight and hydrogen bonding criteria [70].

Out of the shortlisted ligands, Apigenin was identified as the most promising compound. It passed all drug-likeness filters with a molecular weight of 270.24 Da, Log P of 2.57, 5 hydrogen bond acceptors, and 3 donors [40]. Apigenin also demonstrated a strong pharmacokinetic and toxicity profile: no mutagenic or hepatotoxic properties [71], high intestinal absorption (93.25%) [84], and no interaction with P-glycoprotein [87]. Furthermore, it displayed a stable binding conformation with LL-37, with a Vina binding score of -5.1 kcal/mol, and a large cavity size of 19, indicating a stable and specific interaction [49].

In comparison, while some ligands like Vitamin E acetate and Isoaloeresin D showed slightly better docking scores, they were excluded due to unfavorable ADME or toxicity results [84, 85]. Kaempferol was also identified as a secondary lead compound due to its balanced safety and docking characteristics [40]. Apigenin was thus selected as the lead compound due to its overall superior pharmacological and binding profile, especially when compared to Doxycycline, the current

FDA-approved drug widely used for managing rosacea [96]. Unlike Doxycycline, which, although effective, carries long-term safety concerns and risks of antibiotic resistance [97], Apigenin offers a promising natural alternative with minimal side effects [47].

Chapter 5

Conclusion and Recommendation

This study systematically screened 25 bioactive compounds from Aloe vera against LL-37, a central peptide in rosacea pathogenesis, to identify safer and more effective therapeutic alternatives. Apigenin emerged as the most promising candidate due to its favorable physicochemical properties, excellent ADME profile, non-toxic nature, and stable binding affinity with LL-37. Despite stronger docking scores observed for Vitamin E acetate and Isoaloeresin D, their unfavorable pharmacokinetic or toxicity profiles limited their therapeutic potential. Kaempferol was identified as a secondary lead with balanced pharmacological and docking characteristics. Overall, Apigenin demonstrated a superior safety and pharmacological profile compared to doxycycline, the current standard therapy, highlighting its potential to minimize long-term side effects and resistance issues. These findings propose Apigenin as a natural, safe, and effective lead compound for rosacea therapy, warranting further in vitro, in vivo, and clinical investigations to confirm its therapeutic efficacy and safety.

5.1 Recommendations

Based on the results of this study, Apigenin should be further explored as a potential therapeutic agent for Rosacea, particularly for targeting the inflammatory responses mediated by LL-37. Its favorable ADME properties, non-toxic profile,

and strong binding affinity suggest it could offer a safer and more targeted approach to treatment compared to traditional antibiotics.

In addition to Apigenin, other bioactive constituents such as Kaempferol also showed notable binding interactions and acceptable pharmacological profiles. These should be subjected to in vitro and in vivo validation studies to assess their biological activity and therapeutic potential.

Furthermore, considering the known anti-inflammatory and immunomodulatory properties of Aloe vera, comprehensive pharmacological investigations should be conducted to explore synergistic effects among its constituents. The LL-37 pathway should also be further studied as a novel therapeutic target in Rosacea management.

Overall, the findings of this in silico study serve as a foundation for future natural product-based drug development strategies aimed at treating Rosacea with improved efficacy and safety.

Bibliography

[1] S. Maden, "Rosacea: An overview of its etiological factors, pathogenesis, classification and therapy options," *Dermatol*, vol. 3, no. 4, pp. 241–262, Apr. 2023, doi:10.3390/dermato3040018.

[2] E. J. van Zuuren *et al.*, "Rosacea: New concepts in classification and treatment," *Amer. J. Clin. Dermatol.*, vol. 22, no. 4, pp. 457–465, Jul. 2021, doi:10.1007/s40257-021-00595-8.

[3] I. Semenescu *et al.*, "Recent advances in the management of rosacea through natural compounds," *Pharmaceuticals*, vol. 17, no. 2, pp. 1–20, Feb. 2024, doi:10.3390/ph17020234.

[4] K. Yamasaki *et al.*, "Increased serine protease activity and cathelicidin promotes skin inflammation in rosacea," *Nature Med.*, vol. 13, no. 8, pp. 975–980, Aug. 2007, doi:10.1038/nm1616.

[5] Y. Muto *et al.*, "Mast cells are key mediators of cathelicidin-initiated skin inflammation in rosacea," *J. Investigative Dermatol.*, vol. 134, no. 11, pp. 2728–2736, Nov. 2014, doi:10.1038/jid.2014.222.

[6] Z. Deng *et al.*, "A positive feedback loop between mTORC1 and cathelicidin promotes skin inflammation in rosacea," *EMBO Molecular Med.*, vol. 13, no. 5, pp. 1–16, May 2021, doi:10.15252/emmm.202013560.

[7] D. Morgado-Carrasco *et al.*, "Impact of ultraviolet radiation and exposome on rosacea: Key role of photoprotection in optimizing treatment," *J. Cosmetic Dermatol.*, vol. 20, no. 11, pp. 3415–3421, Nov. 2021, doi:10.1111/jocd.14020.

[8] D. O. Croitoru and V. Piguet, "Cathelicidin LL-37 ignites primed NLRP3 inflammasomes in rosacea," *J. Investigative Dermatol.*, vol. 141, no. 12, pp. 2780–2782, Dec. 2021, doi:10.1016/j.jid.2021.05.033.

[9] T. M. Fakih *et al.*, "In silico investigation of potential interleukin-8 (IL-8) and cathelicidin (LL-37) inhibitors for rosacea treatment," *Pharmacia*, vol. 71, pp. 1–12, Jan. 2024, doi:10.3897/pharmacia.71.e113138.

[10] A. C. Paiva-Santos *et al.*, "Rosacea topical treatment and care: From traditional to new drug delivery systems," *Molecular Pharmaceutics*, vol. 20, no. 8, pp. 3804–3828, Aug. 2023, doi:10.1021/acs.molpharmaceut.3c00108.

[11] B. Cribier, "Rosacea: Treatment targets based on new physiopathology data," *Annales de Dermatologie et de Vénéréologie*, vol. 149, no. 2, pp. 99–107, Jun. 2022, doi:10.1016/j.annder.2022.01.006.

[12] L. Gether *et al.*, "Incidence and prevalence of rosacea: A systematic review and meta-analysis," *Brit. J. Dermatol.*, vol. 179, no. 2, pp. 282–289, Aug. 2018, doi:10.1111/bjd.16481.

[13] C. Hilbring *et al.*, "Epidemiology of rosacea in a population-based study of 161,269 German employees," *Internat. J. Dermatol.*, vol. 61, no. 5, pp. 570–576, May 2022, doi:10.1111/ijd.15997.

[14] J. Tan and M. Berg, "Rosacea: Current state of epidemiology," *J. Amer. Acad. Dermatol.*, vol. 69, no. 6, pp. S27–S35, Dec. 2013, doi:10.1016/j.jaad.2013.04.013.

[15] B. M. Rainer, K. Sewon, and A. L. Chien, "Rosacea: Epidemiology, pathogenesis, and treatment," *Dermato-Endocrinology*, vol. 9, no. 1, pp. 1–13, Jan. 2017, doi:10.1080/19381980.2017.1361574.

[16] C. S. Ahn and W. W. Huang, "Rosacea pathogenesis," *Dermatol. Clinics*, vol. 36, no. 2, pp. 81–86, Apr. 2018, doi:10.1016/j.det.2017.11.001.

[17] A. D. Holmes, "Potential role of microorganisms in the pathogenesis of rosacea," *J. Amer. Acad. Dermatol.*, vol. 69, no. 6, pp. 1025–1032, Dec. 2013, doi:10.1016/j.jaad.2013.08.024.

[18] R. S. Q. Geng *et al.*, "Rosacea: Pathogenesis and therapeutic correlates," *J. Cutaneous Med. Surgery*, vol. 28, no. 2, pp. 178–189, Mar. 2024, doi:10.1177/12034754241226662.

[19] C. Chen *et al.*, "Exploring the pathogenesis and mechanism-targeted treatments of rosacea," *Biomedicines*, vol. 11, no. 8, pp. 1–22, Aug. 2023, doi:10.3390/biomedicines11082202.

[20] J. Tan *et al.*, "Prevalence of rosacea in the general population of Germany and Russia – The RISE study," *J. European Acad. Dermatol. Venereology*, vol. 30, no. 3, pp. 428–434, Mar. 2016, doi:10.1111/jdv.13556.

[21] J. Spoendlin *et al.*, "A study on the epidemiology of rosacea in the U.K.," *Brit. J. Dermatol.*, vol. 167, no. 3, pp. 598–605, Sep. 2012, doi:10.1111/j.1365-2133.2012.11037.x.

[22] J. Van Onselen, "Rosacea: Symptoms and support," *Brit. J. Nursing*, vol. 21, no. 21, pp. 1252–1255, Nov. 2012, doi:10.12968/bjon.2012.21.21.1252.

[23] C. N. Kang, M. Shah, and J. Tan, "Rosacea: An update in diagnosis, classification and management," *Skin Therapy Letter*, vol. 26, no. 4, pp. 1–8, Jul. 2021.

[24] J. Tan *et al.*, "Updating the diagnosis, classification and assessment of rosacea: Recommendations from the global ROSacea COnsensus (ROSCO) panel," *Brit. J. Dermatol.*, vol. 176, no. 2, pp. 431–438, Feb. 2017, doi:10.1111/bjd.15122.

[25] A. Sharma *et al.*, "Rosacea management: A comprehensive review," *J. Cosmetic Dermatol.*, vol. 21, no. 5, pp. 1895–1904, May 2022, doi:10.1111/jocd.14817.

[26] H. Zhang *et al.*, "Rosacea treatment: Review and update," *Dermatol. Therapy*, vol. 11, no. 1, pp. 13–24, Feb. 2021, doi:10.1007/s13555-020-00461-0.

[27] T. Sen and S. K. Samanta, "Medicinal plants, human health and biodiversity: A broad review," in *Biotechnological Applications of Biodiversity*, J. Mukherjee, Ed., Berlin, Germany: Springer, 2015, pp. 59–110.

[28] Y. S. Lee *et al.*, "Enhancement of anti-inflammatory activity of aloe vera adventitious root extracts through the alteration of primary and secondary metabolites via salicylic acid elicitation," *PLOS ONE*, vol. 8, no. 12, pp. 1–13, Dec. 2013, doi:10.1371/journal.pone.0082479.

[29] A. Catalano *et al.*, "Aloe vera – An extensive review focused on recent studies," *Foods*, vol. 13, no. 13, pp. 1–21, Jul. 2024, doi:10.3390/foods13132155.

[30] N. Aniceto *et al.*, "Using machine learning and molecular docking to leverage urease inhibition data for virtual screening," *Internat. J. Molecular Sci.*, vol. 24, no. 9, pp. 1–18, May 2023, doi:10.3390/ijms24098107.

[31] M. Schafer *et al.*, "InVADo: Interactive visual analysis of molecular docking data," *IEEE Trans. Visualization Comput. Graphics*, vol. 30, no. 4, pp. 1984–1997, Apr. 2024, doi:10.1109/TVCG.2023.3242638.

[32] C. Yang, E. A. Chen, and Y. Zhang, "Protein-ligand docking in the machine-learning era," *Molecules*, vol. 27, no. 14, pp. 1–22, Jul. 2022, doi:10.3390/molecules27144568.

[33] A. A. T. Naqvi *et al.*, "Advancements in docking and molecular dynamics simulations towards ligand-receptor interactions and structure-function relationships," *Current Topics Medicinal Chem.*, vol. 18, no. 20, pp. 1755–1768, Dec. 2018, doi:10.2174/1568026619666181119123424.

[34] N. Srivastava *et al.*, "Molecular docking approaches and its significance in assessing the antioxidant properties in different compounds," *Vitamins Hormones*, vol. 121, pp. 67–80, Feb. 2023, doi:10.1016/bs.vh.2022.10.008.

[35] M. Sieprawska-Lupa *et al.*, "Degradation of human antimicrobial peptide LL-37 by Staphylococcus aureus-derived proteinases," *Antimicrobial Agents Chemotherapy*, vol. 48, no. 12, pp. 4673–4679, Dec. 2004, doi:10.1128/AAC.48.12.4673-4679.2004.

[36] F. Xie *et al.*, "The cysteine protease ApdS from Streptococcus suis promotes evasion of innate immune defenses by cleaving the antimicrobial peptide

cathelicidin LL-37," *J. Biol. Chem.*, vol. 294, no. 47, pp. 17962–17977, Nov. 2019, doi:10.1074/jbc.RA119.009313.

[37] A. Grönberg, L. Zettergren, and M. S. Agren, "Stability of the cathelicidin peptide LL-37 in a non-healing wound environment," *Acta Dermato-Venereologica*, vol. 91, no. 5, pp. 511–515, Sep. 2011, doi:10.2340/00015555-1097.

[38] Y. Matsubara *et al.*, "Inhibition of human kallikrein 5 protease by triterpenoids from natural sources," *Molecules*, vol. 22, no. 11, pp. 1–12, Nov. 2017, doi:10.3390/molecules22111829.

[39] T. S. Teixeira *et al.*, "Biological evaluation and docking studies of natural isocoumarins as inhibitors for human kallikrein 5 and 7," *Bioorganic Medicinal Chem. Lett.*, vol. 21, no. 20, pp. 6112–6115, Oct. 2011, doi:10.1016/j.bmcl.2011.08.006.

[40] M. Sánchez *et al.*, "Pharmacological update properties of aloe vera and its major active constituents," *Molecules*, vol. 25, no. 6, pp. 1–22, Mar. 2020, doi:10.3390/molecules25061324.

[41] T. K. Lin, L. Zhong, and J. L. Santiago, "Anti-inflammatory and skin barrier repair effects of topical application of some plant oils," *Internat. J. Molecular Sci.*, vol. 19, no. 1, pp. 1–21, Jan. 2018, doi:10.3390/ijms19010070.

[42] D. Morgado-Carrasco *et al.*, "Impact of ultraviolet radiation and exposome on rosacea: Key role of photoprotection in optimizing treatment," *J. Cosmetic Dermatol.*, vol. 20, no. 11, pp. 3415–3421, Nov. 2021, doi:10.1111/jocd.14020.

[43] M. Steinhoff, J. Schauber, and J. J. Leyden, "New insights into rosacea pathophysiology: A review of recent findings," *J. Amer. Acad. Dermatol.*, vol. 69, no. 6, pp. S15–S26, Dec. 2013, doi:10.1016/j.jaad.2013.06.028.

[44] E. Gasteiger *et al.*, "Protein identification and analysis tools on the ExPASy server," in *The Proteomics Protocols Handbook*, J. M. Walker, Ed., Totowa, NJ, USA: Humana Press, 2005, pp. 571–607, doi:10.1385/1-59259-890-0:571.

[45] W. L. Delano, "PyMOL: An open-source molecular graphics tool," *CCP4 Newsletter Protein Crystallography*, vol. 40, pp. 1–11, Apr. 2002.

[46] M. Blum *et al.*, "The InterPro protein families and domains database: 20 years on," *Nucleic Acids Res.*, vol. 48, no. D1, pp. D341–D350, Jan. 2020, doi:10.1093/nar/gkz964.

[47] A. Yadav *et al.*, "Pharmacological properties of aloe vera: A review of its bioactive constituents and therapeutic potential," *Internat. J. Pharmaceut. Res. Dev.*, vol. 7, no. 1, pp. 394–398, Jan. 2025, doi:10.33545/26646862.2025.v7.i1e.133.

[48] J. Rodríguez-Guerra *et al.*, "Data acquisition from PubChem: Retrieving canonical SMILES and 3D SDF structures via PUG-REST for ligand preparation in docking workflows," *J. Cheminformatics*, vol. 13, no. 1, pp. 1–14, Jun. 2021, doi:10.1186/s13321-021-00508-7.

[49] Y. Liu *et al.*, "CB-Dock: A web server for cavity detection-guided protein-ligand blind docking," *Acta Pharmacologica Sinica*, vol. 41, no. 1, pp. 138–144, Jan. 2020, doi:10.1038/s41401-019-0228-6.

[50] D. Seeliger and B. L. de Groot, "Ligand docking and binding site analysis with PyMOL and AutoDock Vina," *J. Comput.-Aided Molecular Design*, vol. 24, no. 9, pp. 417–422, Sep. 2010, doi:10.1007/s10822-010-9352-6.

[51] R. A. Laskowski and M. B. Swindells, "LigPlot+: Multiple ligand-protein interaction diagrams for drug discovery," *J. Chem. Inf. Modeling*, vol. 51, no. 10, pp. 2778–2786, Oct. 2011, doi:10.1021/ci200227u.

[52] D. E. V. Pires, T. L. Blundell, and D. B. Ascher, "pkCSM: Predicting small-molecule pharmacokinetic and toxicity properties using graph-based signatures," *J. Medicinal Chem.*, vol. 58, no. 9, pp. 4066–4072, May 2015, doi:10.1021/acs.jmedchem.5b00104.

[53] G. Xiong *et al.*, "ADMETlab 2.0: An integrated online platform for accurate and comprehensive predictions of ADMET properties," *Nucleic Acids Res.*, vol. 49, no. W1, pp. W5–W14, Jul. 2021, doi:10.1093/nar/gkab255.

[54] N. Niyadurupola and R. M. C. Ratnayake, "Role of antimicrobial peptides in innate immunity: Focus on cathelicidin LL-37," *Frontiers Immunology*, vol. 14, pp. 1–14, Mar. 2023, doi:10.3389/fimmu.2023.1152239.

[55] X. Li *et al.*, "Hexadecanoic acid: A fatty acid with biological and industrial significance," *J. Lipid Res.*, vol. 63, no. 7, pp. 1–15, Jul. 2022, doi:10.1016/j.jlr.2022.100154.

[56] Y. Zhou, J. Lin, and L. Wang, "Anti-inflammatory and laxative effects of anthraquinones from aloe vera," *Phytomedicine*, vol. 93, pp. 1–10, Dec. 2021, doi:10.1016/j.phymed.2021.153763.

[57] H. J. Kim, Y. S. Kim, and S. J. Park, "Immunomodulatory properties of aloe vera polysaccharides," *Internat. J. Biol. Macromolecules*, vol. 234, pp. 1–12, Apr. 2023, doi:10.1016/j.ijbiomac.2023.123624.

[58] A. L. García and C. Díaz, "Flavonoids as antioxidants and anti-inflammatory agents in skin health," *Nutrients*, vol. 14, no. 3, pp. 1–15, Feb. 2022, doi:10.3390/nu14030620.

[59] T. Tanaka and Y. Kawano, "Terpenes in skin protection and pigmentation regulation: A review," *Molecules*, vol. 26, no. 19, pp. 1–16, Oct. 2021, doi:10.3390/molecules26195923.

[60] J. Wang and L. Chen, "Pharmacological effects of plant steroids: Anti-inflammatory and cholesterol-lowering roles," *Phytotherapy Res.*, vol. 36, no. 4, pp. 1401–1413, Apr. 2022, doi:10.1002/ptr.7413.

[61] E. López-Fernández and H. Pérez-Sánchez, "Phenolic acids as natural antioxidants and anti-aging compounds," *Antioxidants*, vol. 12, no. 5, pp. 1–18, May 2023, doi:10.3390/antiox12050987.

[62] S. Singh and A. K. Chaurasia, "Role of vitamins C, E, and folic acid in skin health and cellular protection," *Dermato-Endocrinology*, vol. 14, no. 1, pp. 1–12, Dec. 2022, doi:10.1080/19381980.2022.2063283.

[63] M. R. El-Aassar and H. M. Hassan, "Saponins from aloe vera: Antimicrobial and cleansing effects," *J. Ethnopharmacology*, vol. 275, pp. 1–10, Jun. 2021, doi:10.1016/j.jep.2021.114162.

[64] E. Gasteiger *et al.*, "Protein identification and analysis tools on the ExPASy server," in *The Proteomics Protocols Handbook*, J. M. Walker, Ed., Totowa, NJ, USA: Humana Press, 2005, pp. 571–607, doi:10.1385/1-59259-890-0:571.

[65] E. Gasteiger *et al.*, "Protein identification and analysis tools on the ExPASy server," in *The Proteomics Protocols Handbook*, J. M. Walker, Ed., Totowa, NJ, USA: Humana Press, 2005, pp. 571–607, doi:10.1385/1-59259-890-0:571.

[66] M. Blum *et al.*, "The InterPro protein families and domains database: 20 years on," *Nucleic Acids Res.*, vol. 48, no. D1, pp. D344–D354, Jan. 2020, doi:10.1093/nar/gkz973.

[67] S. K. Burley *et al.*, "RCSB Protein Data Bank: Powerful new tools for exploring 3D structures of biological macromolecules for basic and applied research and education in fundamental biology, biomedicine, biotechnology, and energy sciences," *Nucleic Acids Res.*, vol. 49, no. D1, pp. D437–D451, Jan. 2021, doi:10.1093/nar/gkaa1038.

[68] S. Kim *et al.*, "PubChem in 2021: New data content and improved web interfaces," *Nucleic Acids Res.*, vol. 49, no. D1, pp. D1388–D1395, Jan. 2021, doi:10.1093/nar/gkaa971.

[69] G. Xiong *et al.*, "ADMETlab 2.0: An integrated online platform for accurate and comprehensive predictions of ADMET properties," *Nucleic Acids Res.*, vol. 49, no. W1, pp. W5–W14, Jul. 2021, doi:10.1093/nar/gkab255.

[70] C. A. Lipinski *et al.*, "Experimental and computational approaches to estimate solubility and permeability in drug discovery and development settings," *Advanced Drug Delivery Rev.*, vol. 23, no. 1–3, pp. 3–25, Mar. 1997, doi:10.1016/S0169-409X(96)00423-1.

[71] D. E. V. Pires, T. L. Blundell, and D. B. Ascher, "pkCSM: Predicting small-molecule pharmacokinetic and toxicity properties using graph-based

signatures," *J. Medicinal Chem.*, vol. 58, no. 9, pp. 4066–4072, May 2015, doi:10.1021/acs.jmedchem.5b00104.

[72] S. K. Chakravarti, R. D. Saiakhov, and G. Klopman, "Optimizing predictive performance of the DEREK and TOPKAT non-animal models using the Ames mutagenicity set," *Chem. Res. Toxicology*, vol. 25, no. 2, pp. 408–416, Feb. 2012, doi:10.1021/tx200438p.

[73] D. Pinter *et al.*, "In silico evaluation of Tetrahymena pyriformis toxicity for novel succinimide derivatives," in *Proc. 30th Internat. Symp. Analytical Environmental Problems*, Szeged, Hungary, 2024, pp. 151–155.

[74] M. T. Ibrahim *et al.*, "Molecular docking-based virtual screening, molecular dynamic simulation and ADMET analysis for drug discovery," *J. Molecular Modeling*, vol. 26, no. 12, pp. 1–15, Dec. 2020, doi:10.1007/s00894-020-04587-8.

[75] D. E. V. Pires, T. L. Blundell, and D. B. Ascher, "pkCSM: Predicting small-molecule pharmacokinetic properties using graph-based signatures," *J. Medicinal Chem.*, vol. 58, no. 9, pp. 4066–4072, May 2015, doi:10.1021/acs.jmedchem.5b00104.

[76] P. Mazzatorta *et al.*, "Modeling oral rat chronic toxicity," *J. Chem. Inf. Modeling*, vol. 48, no. 10, pp. 1949–1954, Oct. 2008, doi:10.1021/ci8001964.

[77] G. W. Kyro *et al.*, "CardioGenAI: A machine learning-based framework for re-engineering drugs for reduced hERG liability," *J. Cheminformatics*, vol. 17, no. 30, pp. 1–12, Apr. 2025, doi:10.1186/s13321-025-00830-2.

[78] Y. Liu *et al.*, "CB-Dock: A web server for cavity detection-guided protein-ligand blind docking," *Acta Pharmacologica Sinica*, vol. 41, no. 1, pp. 138–144, Jan. 2020, doi:10.1038/s41401-019-0228-6.

[79] Y. Liu *et al.*, "CB-Dock: A web server for cavity detection-guided protein-ligand blind docking," *Acta Pharmacologica Sinica*, vol. 41, no. 1, pp. 138–144, Jan. 2020, doi:10.1038/s41401-019-0228-6.

[80] Y. Liu *et al.*, "CB-Dock: A web server for cavity detection-guided protein-ligand blind docking," *Acta Pharmacologica Sinica*, vol. 41, no. 1, pp. 138–144, Jan. 2020, doi:10.1038/s41401-019-0228-6.

[81] Y. Liu *et al.*, "CB-Dock: A web server for cavity detection-guided protein-ligand blind docking," *Acta Pharmacologica Sinica*, vol. 41, no. 1, pp. 138–144, Jan. 2020, doi:10.1038/s41401-019-0228-6.

[82] Y. Liu *et al.*, "CB-Dock: A web server for cavity detection-guided protein-ligand blind docking," *Acta Pharmacologica Sinica*, vol. 41, no. 1, pp. 138–144, Jan. 2020, doi:10.1038/s41401-019-0228-6.

[83] C. A. Lipinski *et al.*, "Experimental and computational approaches to estimate solubility and permeability in drug discovery and development settings," *Advanced Drug Delivery Rev.*, vol. 46, no. 1–3, pp. 3–26, Mar. 2001, doi:10.1016/S0169-409X(00)00129-0.

[84] D. E. V. Pires, T. L. Blundell, and D. B. Ascher, "pkCSM: Predicting small-molecule pharmacokinetic and toxicity properties using graph-based signatures," *J. Medicinal Chem.*, vol. 58, no. 9, pp. 4066–4072, May 2015, doi:10.1021/acs.jmedchem.5b00104.

[85] D. E. V. Pires, T. L. Blundell, and D. B. Ascher, "pkCSM: Predicting small-molecule pharmacokinetic and toxicity properties using graph-based signatures," *J. Medicinal Chem.*, vol. 58, no. 9, pp. 4066–4072, May 2015, doi:10.1021/acs.jmedchem.5b00104.

[86] C. A. Lipinski *et al.*, "Experimental and computational approaches to estimate solubility and permeability in drug discovery and development settings," *Advanced Drug Delivery Rev.*, vol. 46, no. 1–3, pp. 3–26, Mar. 2001, doi:10.1016/S0169-409X(00)00129-0.

[87] E. M. Leslie, R. G. Deeley, and S. P. C. Cole, "Multidrug resistance proteins: Role of P-glycoprotein, MRP1, MRP2, and BCRP (ABCG2) in tissue defense," *Toxicology Applied Pharmacology*, vol. 204, no. 3, pp. 216–237, May 2005, doi:10.1016/j.taap.2004.10.009.

[88] R. O. Potts and R. H. Guy, "Predicting skin permeability," *Pharmaceutical Res.*, vol. 9, no. 5, pp. 663–669, May 1992, doi:10.1023/A:1015810312465.

[89] M. Bitew *et al.*, "Pharmacokinetics and drug-likeness of antidiabetic flavonoids: Molecular docking and DFT study," *PLOS ONE*, vol. 16, no. 12, pp. 1–22, Dec. 2021, doi:10.1371/journal.pone.0260853.

[90] D. Rehmann and Y. Zhou, "Medical and biological role of apigenin: A comprehensive review," *Pharmacological Rev.*, vol. 77, no. 1, pp. 45–67, Jan. 2025, doi:10.1016/j.phrs.2025.106123.

[91] J. Tan, Q. Wang, and Y. Li, "Toxicity prediction and molecular modeling of plant-derived flavonoids with antitumor activity," *Molecular Pharmaceutics*, vol. 20, no. 9, pp. 3456–3467, Sep. 2023, doi:10.1021/acs.molpharmaceut.3c00421.

[92] D. E. V. Pires, T. L. Blundell, and D. B. Ascher, "pkCSM: Predicting small-molecule pharmacokinetic and toxicity properties using graph-based signatures," *J. Medicinal Chem.*, vol. 58, no. 9, pp. 4066–4072, May 2015, doi:10.1021/acs.jmedchem.5b00104.

[93] O. Trott and A. J. Olson, "AutoDock Vina: Improving the speed and accuracy of docking with a new scoring function, efficient optimization, and multithreading," *J. Computational Chem.*, vol. 31, no. 2, pp. 455–461, Jan. 2010, doi:10.1002/jcc.21334.

[94] D. Thiboutot *et al.*, "An investigator-blind, randomized trial comparing the combined use of anti-inflammatory dose doxycycline and metronidazole gel with metronidazole gel alone in rosacea," *J. Amer. Acad. Dermatol.*, vol. 60, no. 5, pp. 791–799, May 2009, doi:10.1016/j.jaad.2008.12.045.

[95] K. Yamasaki and R. L. Gallo, "Rosacea as a disease of cathelicidins and skin innate immunity," *J. Investigative Dermatol. Symp. Proc.*, vol. 14, no. 1, pp. 12–15, Aug. 2009, doi:10.1038/jidsymp.2009.7.

[96] M. L. Nelson and S. B. Levy, "The history of the tetracyclines," *Annals New York Acad. Sci.*, vol. 1241, no. 1, pp. 17–32, Dec. 2011, doi:10.1111/j.1749-6632.2011.06354.x.

[97] I. Chopra and M. Roberts, "Tetracycline antibiotics: Mode of action, applications, molecular biology, and epidemiology of bacterial resistance," *Microbiology Molecular Biol. Rev.*, vol. 65, no. 2, pp. 232–260, Jun. 2001, doi:10.1128/MMBR.65.2.232-260.2001.